



Universitat
de les Illes Balears

Title: Predicting meteotsunamis in Ciutadella: BRIFS model evaluation for recent events and potential of ensemble forecasting

AUTHOR: Albert Buils Casasnovas

Master's Thesis

Master's degree in Advanced Physics and Applied Mathematics
(With a speciality/Itinerary Geophysical Fluids)

at the

UNIVERSITAT DE LES ILLES BALEARS

Academic year: 2018-2019

Date 31 July 2019

UIB Master's Thesis Supervisor: Baptiste Mourre

UIB Master's Thesis Co-Supervisor: Romualdo Romero March

Contents

1	Introduction	3
1.1	Context	3
1.1.1	Meteotsunamis	3
1.1.2	Amplification processes	3
1.1.3	SOCIB	7
1.2	Objectives	7
2	Methodology and Data	8
2.1	Data	8
2.1.1	SOCIB data	8
2.1.2	PortsIB data through Geonica web portal	9
2.2	Satellite images	9
2.3	Balearic Rissaga Forecasting System	10
2.3.1	BRIFS configuration: WRF and ROMS models	10
2.3.2	ROMS validation	13
2.3.3	WRF parameterizations	15
3	Rissaga characterisation: past cases	18
3.1	15-June-2006 (~ 4 m)	19
3.2	25-May-2008 (~ 1.65 m)	20
3.3	18-August-2014 (1.45 m)	22
3.4	22-April-2015 (1.4 m)	23
3.5	01-August-2015 (1.35 m)	25
3.6	01-April-2016 (1.24 m)	26
3.7	16-July-2018 (1.49 m)	27
3.8	Synthesis	28
4	WRF sensitivity experiments	29
4.1	Toward the ensemble prediction	32
4.2	Model ensemble evaluation	34
4.2.1	June 15, 2006	35
4.2.2	August 18, 2014	36
4.2.3	July 16, 2018	38
5	Conclusions	41
6	Future work	42

1 Introduction

1.1 Context

1.1.1 Meteotsunamis

Meteotsunamis are sea level oscillations with large amplitude and short period that occur in closed basins or inlets. Here in the Balearic Islands this phenomena is known as "rissaga" (*Tintoré et al.*, 1988). This kind of events occur mainly in summer and it usually doesn't cause major problems for the users of the harbour. However, some extreme events occasionally occur in Ciutadella harbour causing major problems for the users of the harbour, including boat sinking, restaurant flooding, etc. The greatest rissaga in the last twenty years happened on June 15, 2006. This rissaga will be explained later.

Meteotsunamis are similar to tsunamis but they differ in its generation. While a tsunami is generated by an earthquake or an underwater volcanic eruption, meteotsunamis are generated by an atmospheric disturbance (*Montserrat et al.*, 2006a). In the case of Ciutadella, this forcing triggers sea level oscillations which travel through the Menorca channel. The effects of the rissaga are only observed inside the harbour. While inside the harbour the sea level oscillations can reach 1.5-2 meters height, these oscillations are hard to detect outside the harbour where they reach a few tens of cm as maximum. This is due to the characteristics of the harbour and a particular resonance effect.

This phenomenon results from several amplification processes that occur during the propagation of the pressure disturbance which begins over the channel and ends at Ciutadella.

1.1.2 Amplification processes

The atmospheric disturbance that induces the extreme rissaga starts with small-scale oscillations of a few hPa that are translated in a few centimetres in the ocean as the result of the inverse barometer effect. During its propagation through the Menorca channel, inside the harbour these few centimetres are amplified up to 1 or 2 metres, or even 4 m in the case of the 15 June 2006 rissaga. There are three amplification factors during the propagation (*Montserrat et al.*, 2006b). The first one happens during the propagation between Mallorca and Menorca, along the Menorca channel, and it is caused by a resonant effect. It is followed by a shelf amplification. And finally the biggest amplification is caused by the resonance inside the harbour.

- **Proudman resonance (In Menorca channel).** The Proudman resonance (*Proudman*, 1929) is a resonant response of a water body (in shallow waters) to an atmospheric distur-

bance. When the velocity of this atmospheric disturbance matches the barotropic water wave velocity then the sea level oscillations are amplified. The water wave velocity is $c = \sqrt{gH}$ where g is the gravity constant, and H is the depth on the water column. For our particular case (Menorca channel) this velocity is around 27 m/s. So when the atmospheric disturbance travels with a speed close to this, the magnitude of the sea level oscillations are amplified. This effect is shown in figure 1.1.2 .

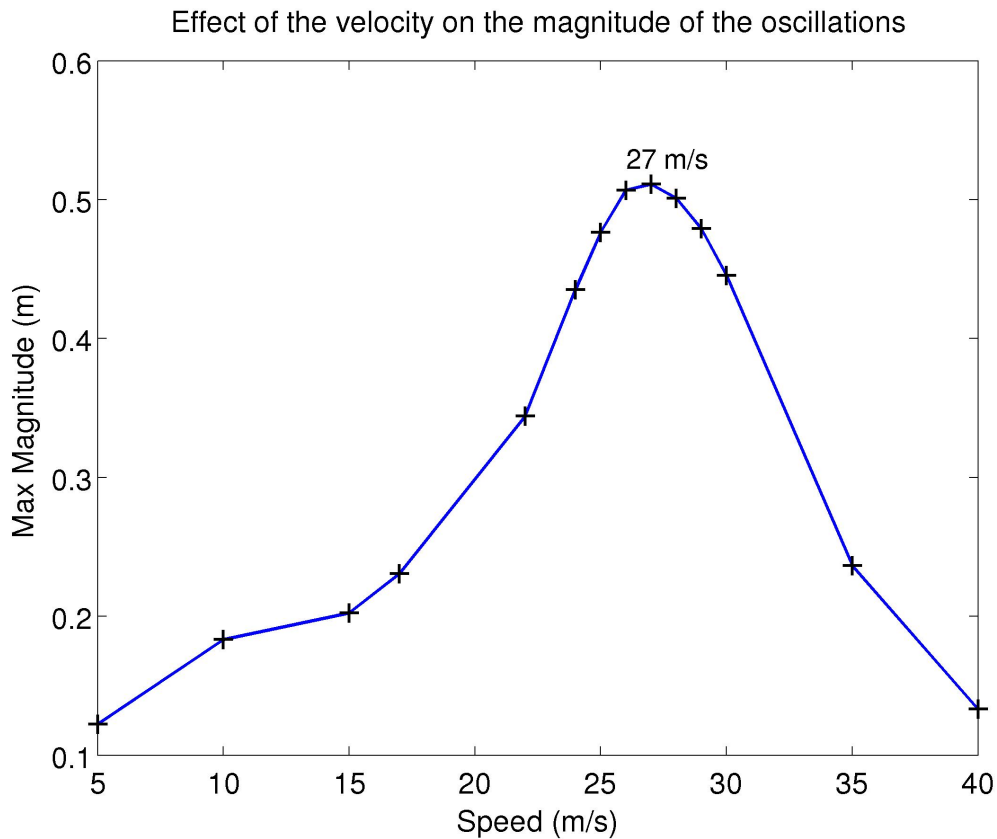


Figure 1: Experiment made to see the influence of the atmospheric pressure disturbance speed on the magnitude of the sea level induced oscillations in the Menorca channel.

This experiment was made by forcing a shallow water toy model (with an idealised channel with the mean depth of the Menorca channel) with a synthetic atmospheric disturbance (a sinusoidal forcing with 2 hPa amplitude) propagating in the direction of the channel. Here we can see that as the speed gets close to c , we reach a maximum. This is the effect of the Proudman resonance. Due to this resonance the oscillations of a few centimetres turn to oscillations of 20 to 30 centimetres (in the figure it is an ideal case, without any force that weakens the wave, for this reason it reaches up to 55 cm).

- **Shelf Amplification.** This amplification is caused by the sloping bathymetry. As it was

said before, the speed of the oceanic wave is $c = \sqrt{gH}$, so when the wave gets close to the coast its kinetic energy is reduced due to the decrease of depth. This loss in kinetic energy produces an increase in potential energy. Consequently, the height of the wave also increases. This amplification was explained by George Green. Basically, the Green's law describes how the non-breaking surface gravity waves propagate through a variable depth and width in shallow water (*Green*, 1838). This law states the relation:

$$H_1 \sqrt[4]{h_1} = H_2 \sqrt[4]{h_2} \quad (1)$$

where H_1 and H_2 are the wave heights at two different locations where the wave passes, and h_1 and h_2 are the mean water depths at the same two locations. An ideal case where the spatial variations of the wave height H for travelling waves in water of mean h and width b satisfies

$$H \sqrt{b} \sqrt[4]{h} \quad (2)$$

So, when the depth decreases by a factor sixteen, the waves become twice as high.

Taking into account that the channel of Menorca has a mean depth of ~ 80 m, the propagated waves approximately double their height when reaching the harbour entrance, which has a mean depth of $\sim 4.5 - 5$ m, .

- **Harbour resonance (Seiches).** The last amplification that occurs during the rissaga process is the strongest one. This amplification is caused by the geometry of the harbour (*Rabinovich*, 2012). To understand this resonances the seiche concept must be introduced. Seiches are long-period waves in closed or semi-closed basins, which oscillate at the normal oscillation modes of the harbour. These normal modes depend on the geometry and depth of the harbour. These normal modes are antisymmetrical and the maximum sea level oscillations occur at the end of the harbour (it always has a node in the harbour entrance).

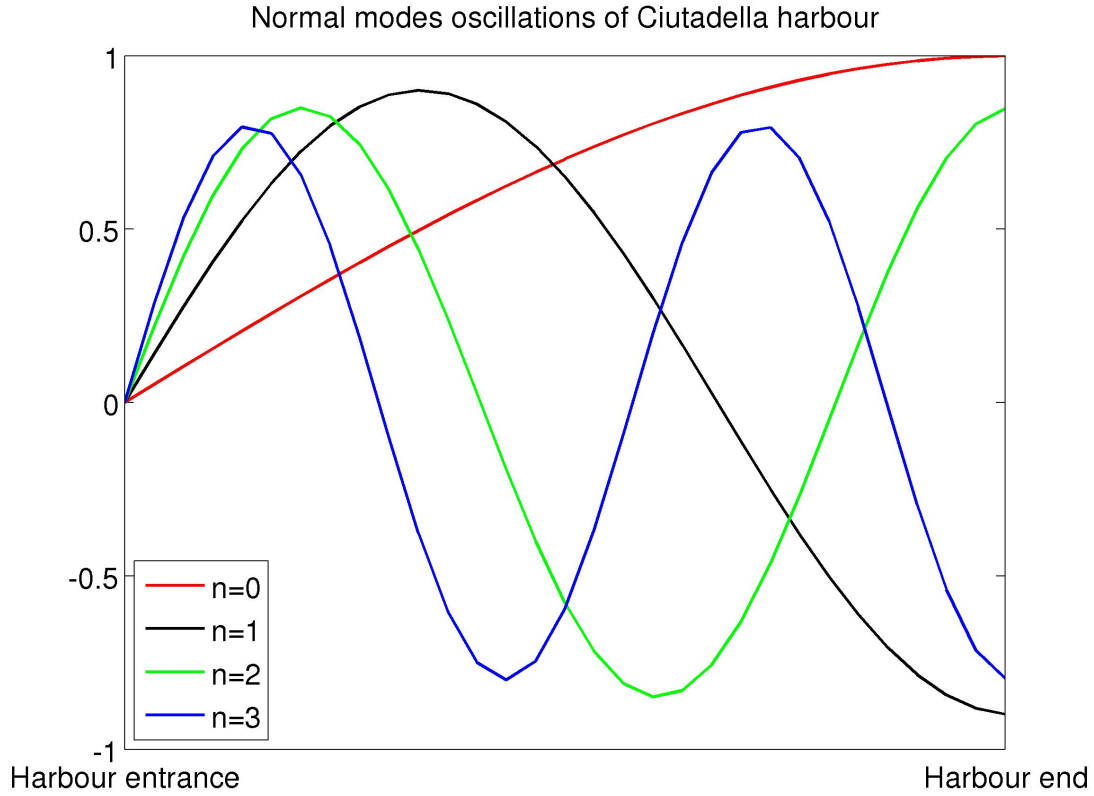


Figure 2: The first four normal modes. The amplitude of the modes is attenuated as n grows. The maximum amplitudes are achieved by the fundamental mode.

When the period of these movements coincides with the natural period of influence, resonance occurs. The mode which triggers the greatest sea level oscillations is the fundamental mode. For bays and ports where entry is narrow (the case of Ciutadella) this mode is dominant and the fundamental periods can be approximated by the following expression (*Rabinovich, 2012*):

$$T_n = \frac{4L}{(2n+1)\sqrt{gH}} \quad (3)$$

where L is the length of the harbour, H is the mean depth of the harbour and g is the gravity constant. This expression can be used to calculate the fundamental period of Ciutadella. Supposing that the harbour length is around 1 km and the mean depth is 4.5 m, then the fundamental period, calculated with the expression 3, is 10.64 min. This result is similar to the one obtained by (*Monserrat et al., 2006b*) which is about 10.5 min.

1.1.3 SOCIB

The Balearic Islands Coastal Observing and Forecasting System (SOCIB) is a multiplatform, distributed and integrated system, a scientific and technological infrastructure that supports operational oceanography in a Mediterranean and international framework.

Its main goal is to develop an observing and forecasting system that provides free, open, quality-controlled, and timely streams of data in order to achieve 3 objectives.

- Support research and technology development.
- Support longer-term strategic needs from society in the context of global change.
- Strengthen operational oceanography in the Balearic Islands and in Spain

SOCIB is structured in three main divisions, the observing, forecasting and data center components. These are supported by the Engineering and Technology Development Division (ETD division).

The observing facilities is divided in six main facilities: a catamaran research vessel; HF radar at Ibiza channel; A fleet of gliders; Lagrangian platform; Fixed stations and Beach monitoring facilities. Moreover, the Modelling Facility is responsible for the generation and operation of numerical simulations and predictions. This thesis has been developed within the Modelling and Forecasting Facility. The preoperational rissaga forecasting system was implemented during 2011-2012. It was then rewritten and set up in its present form in May 2015.

1.2 Objectives

Two main objectives are addressed in this thesis. The first one is the classification of the largest rissaga events of the last years and the description of their generation mechanisms. This classification has been carried out studying satellite images and pressure time series from barometers.

The second main objective was to investigate the model sensitivity modifying the physical parameterizations of the WRF atmospheric model, and to evaluate the performance of these ensembles of simulations to improve the rissaga forecasting.

2 Methodology and Data

2.1 Data

Barometers are essential instruments to investigate rissagas due to the atmospheric origin of the phenomena.

Issuing a warning from barometer observation only, is challenging. The reason is that the disturbance may travel with a speed of 20-30 m/s and there is only a very short time to warn the population about the upcoming risk when the first barometer registers the existence of atmospheric disturbances. Furthermore, the coupling between the atmospheric disturbance and the ocean can occur within a few tens of kilometers from Ciutadella inlet.

In this thesis, data from the SOCIB observation network has been used, more concretely a series of barometers and tide gauges in addition to data from <http://webtrans.geonica.com>, which compiles the observations collected by PortsIB instruments in Ciutadella. As all cases treated in this work are run in hindcast mode (past events), some satellite images (<http://www.sat.dundee.ac.uk>) are also used to try to classify the different cases of rissaga.

2.1.1 SOCIB data

As mentioned before, SOCIB observational network is composed by barometers and tide gauges distributed across all the Balearic Islands, some of them installed in collaboration with other institutions (Portsib, IMEDEA, Govern,...). All these data are freely accessible and can be found on the SOCIB website in the Data Center Facility (<http://socib.es/?seccion=dataCenter>). In figure 3 the localisation of the different instruments in the Balearic Islands is shown.

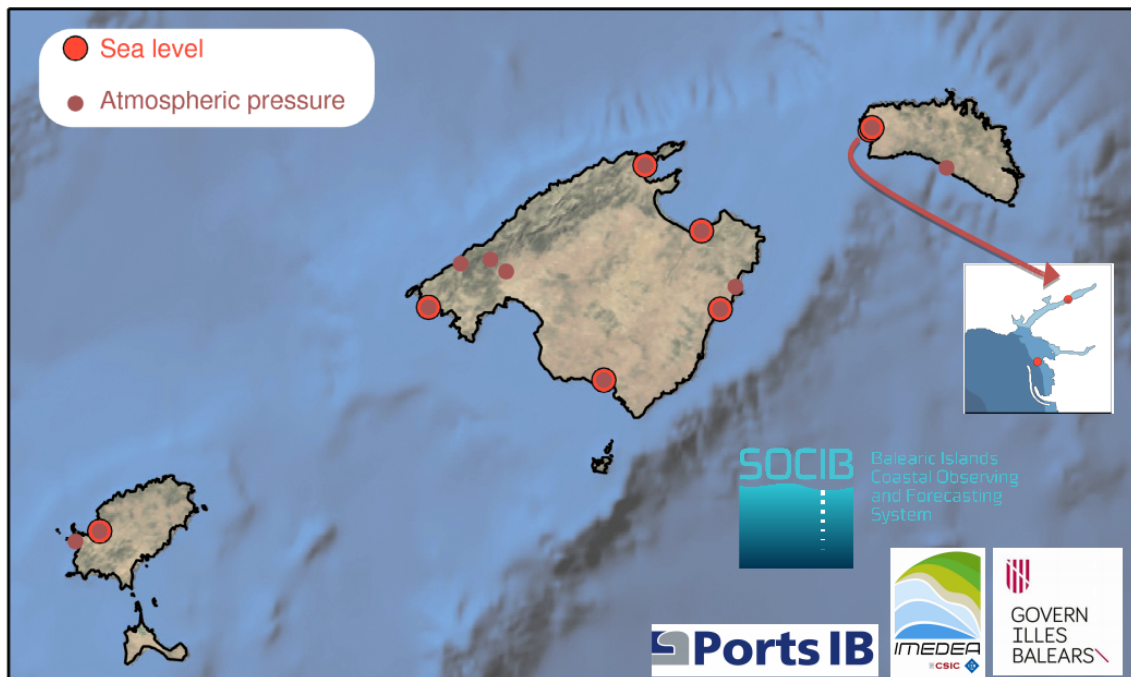


Figure 3: Localization of the barometers and tide gauges from SOCIB.

With regard to meteorological instruments the data collection period dates back to 2011, with short periods during which some of the instruments did not work. The sampling interval of the barometers is 30 seconds, while the tide gauges is 1 min.

2.1.2 PortsIB data through Geonica web portal

SOCIB's tide gauge in Ciutadella was accidentally removed during a solidarity cleaning of the inlet in October, 2018. Since that day, the only instrument that measured the sea level oscillations in Ciutadella's inlet is the tide gauge provided by Ports IB. Ports IB operates a tide gauge in Ciutadella harbour. These data are distributed in <http://webtrans.geonica.com/>, together with information from temperature, pressure, wind direction etc

2.2 Satellite images

For the rissaga characterisation some satellite images are used. These images are taken from the web page <http://www.sat.dundee.ac.uk/>. The images used are from the Mid-IR/ water vapour channel of the Meteosat SEVIRI. For the dates before 2015 only images every 6 hours are available. For the recent events images are provided every hour.

2.3 Balearic Rissaga Forecasting System

The predictability of the meteotsunamis is a difficult challenge due to the complexity of the process. The small-scale oscillations that produce the meteotsunamis are very difficult to reproduce in the simulations. Also, the coupling between the atmospheric disturbance and the ocean is a key factor to take into account. The fact that it is difficult to know the exact moment when the coupling is produced, due to the lack of information along the channel, is an added problem in order to make an operational prediction.

The Balearic Rissaga Forecasting System (BRIFS) is the model which has been developed at SOCIB [*Renault et al. (2011)*, *Licer et al. (2017)*]. It aims to quantitatively predict the occurrence of extreme sea level oscillations associated with meteotsunamis in the Menorcan harbour of Ciutadella. It is based on the combination of both atmospheric and oceanic models. This system is able to reproduce the main features that take place during the rissaga event. A 48-h prediction of air pressure disturbances and associated sea level response over the Balearic shelf and in Ciutadella harbour is updated every day on SOCIB website (www.socib.es).

This system aims at supporting and complementing the AEMET (Agencia Estatal de Meteorología) rissaga alert mainly based on the examination of the synoptic conditions of the atmosphere.

The BRIFS also complements the new system recently implemented by the group of meteorology of the University of the Balearic Islands, based on ensembles of idealized simulations *Romero et al. (2019)*. This other system is based on capturing the key physical processes that induce the meteotsunamis with a low computational cost. It includes the simulation of the genesis of the atmospheric pressure disturbance and the propagation of the gravity waves. These gravity waves are synthetically triggered using a 2D nonhydrostatic fully compressible model within a vertical environment provided by a representative sounding. It also simulates the oceanic response by solving a shallow-water model applied to an idealized 80 m depth channel and an idealized 5 m depth inlet.

2.3.1 BRIFS configuration: WRF and ROMS models

The Weather Research and Forecasting model (WRF) is a next-generation mesoscale numerical weather prediction system designed for both atmospheric research and operational forecasting

applications

(<https://www.mmm.ucar.edu/weather-research-and-forecasting-model>). It features two dynamical cores, a data assimilation system, and a software architecture supporting parallel computation and system extensibility. It is a fully compressible nonhydrostatic equation model, with complete Coriolis and curvature terms. It uses mass-based terrain-following coordinate and the vertical grid-spacing can vary with height. For the horizontal coordinates it uses Arakawa C-grid staggering. It conserves the scalar fluxes form for prognostic variables and it also has 2nd to 6th order advection options both vertical and horizontal.

In the BRIFS configuration, WRF is implemented in a two-nested-grid configuration over the Western Mediterranean basin, with a larger domain with a grid resolution of 20km and a inner domain with a grid resolution of 4 km over an area around the Balearic Islands extending to the South until the Algerian coast. As discussed above, the integration of the vertical levels (ninety-seven in our case) is made with a finer resolution in the lower levels in order to reproduce with more precision the atmospheric characteristics associated with the Rissaga phenomena. Initial state and boundary conditions are prescribed from the synoptic atmospheric conditions described by the GDAS/GFS analysis/forecast, or FNL (for BRIFS hindcasts), from the National Centers for Environmental Prediction (NCEP).

WRF air pressure outputs with a 2-minute temporal resolution are used to force a the Regional Ocean Modelling System (ROMS) (<https://www.myroms.org/>). ROMS is a free-surface, terrain following, primitive equations ocean model with Boussinesq and hydrostatic approximations. It also includes several vertical mixing schemes, multiple levels of nesting and composed grids. The hydrostatic primitive equations for momentum are solved using split-explicit time-stepping scheme which requires special treatment and coupling between barotropic and baroclinic modes. All 2D and 3D equations are time-discretized using a third order accurate predictor (Leap-frog) and corrector (Adams-Molten) time-stepping algorithm. In the vertical, the primitive equations are discretized over variable topography using stretched terrain following coordinates. In the horizontal, the primitive equations are evaluated using boundary-fitted, orthogonal curvilinear coordinates on staggered Arkawa C-grid. Due to the 2-dimensional nature of the processes involved in the build-up of the rissaga, BRIFS does not consider any density stratification.

ROMS is implemented in the BRIFS model using a two-nested grid configuration, where the larger domain (parent) is forced by 2-min WRF air pressure. This larger domain covers the

Balearic Islands with a horizontal resolution of 1km and it provides the boundary conditions to the inner domain (child). The inner domain covers the area around Ciutadella with a spatial resolution of 10m. Figure 2.3.1 illustrates the BRIFS configuration.

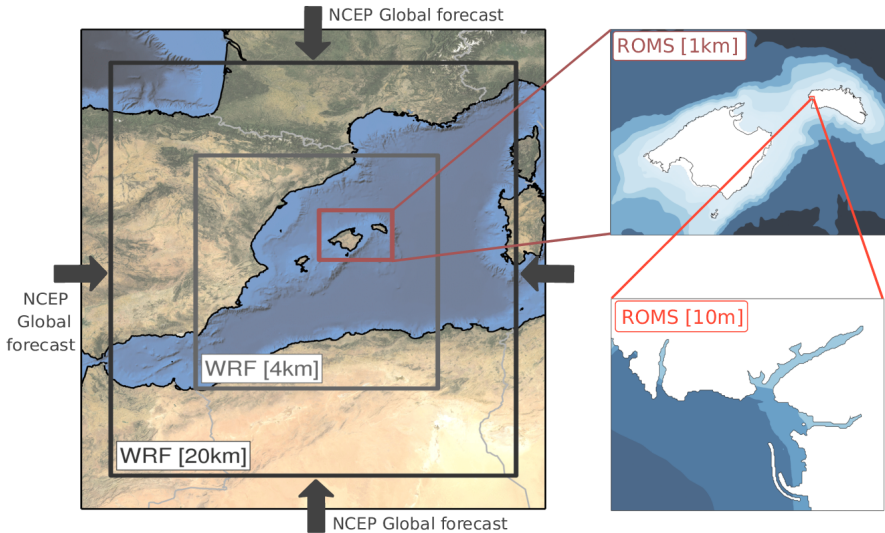


Figure 4: BRIFS configuration (www.socib.es).

BRIFS uses a 12-hour spinup period for the WRF model before starting the prediction at 00:00 UTC every day. NCEP prediction fields are provided every 3 hours at WRF boundaries. The ROMS simulation is first run on the coarser grid using the outputs of the WRF prediction. Then, ROMS forecast is produced on the finer grid using both WRF sea level pressure predictions and ROMS coarser simulation outputs at the lateral boundaries.

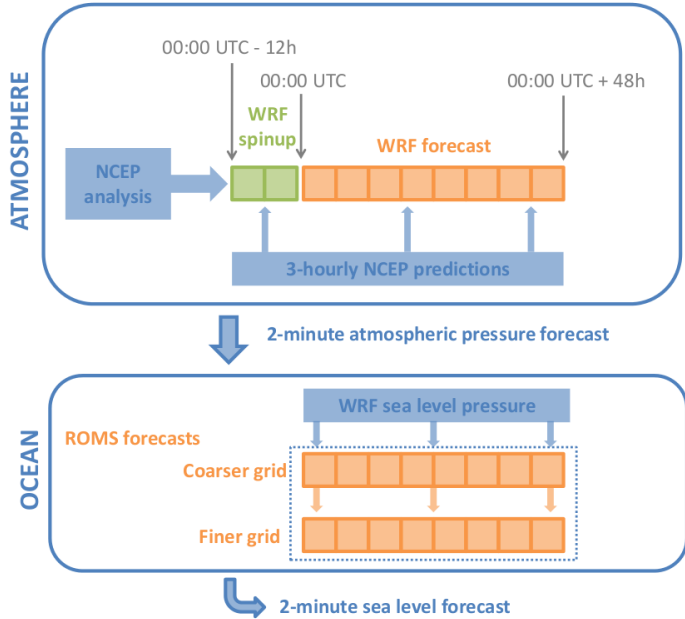


Figure 5: BRIFS forecast production (www.socib.es).

The different steps involved in the BRIFS prediction are shown in figure 5

2.3.2 ROMS validation

This thesis has mainly focused on the atmospheric part of the BRIFS model, since the ROMS model has been validated in previous studies. As an illustration, one of the validation exercises consisted in forcing the model with a pressure field obtained from observations and studying the response of the oceanic model.

In order to carry out this validation a synthetic forcing was made using observed pressure time series (Baptiste Mourre and Lola Gautreau, *Gautreau (2018)*) for a particular case of rissaga that occurred on 18 July, 2018. A clear propagation of the atmospheric disturbance was observed in the different barometers mentioned earlier in 2.1.1.

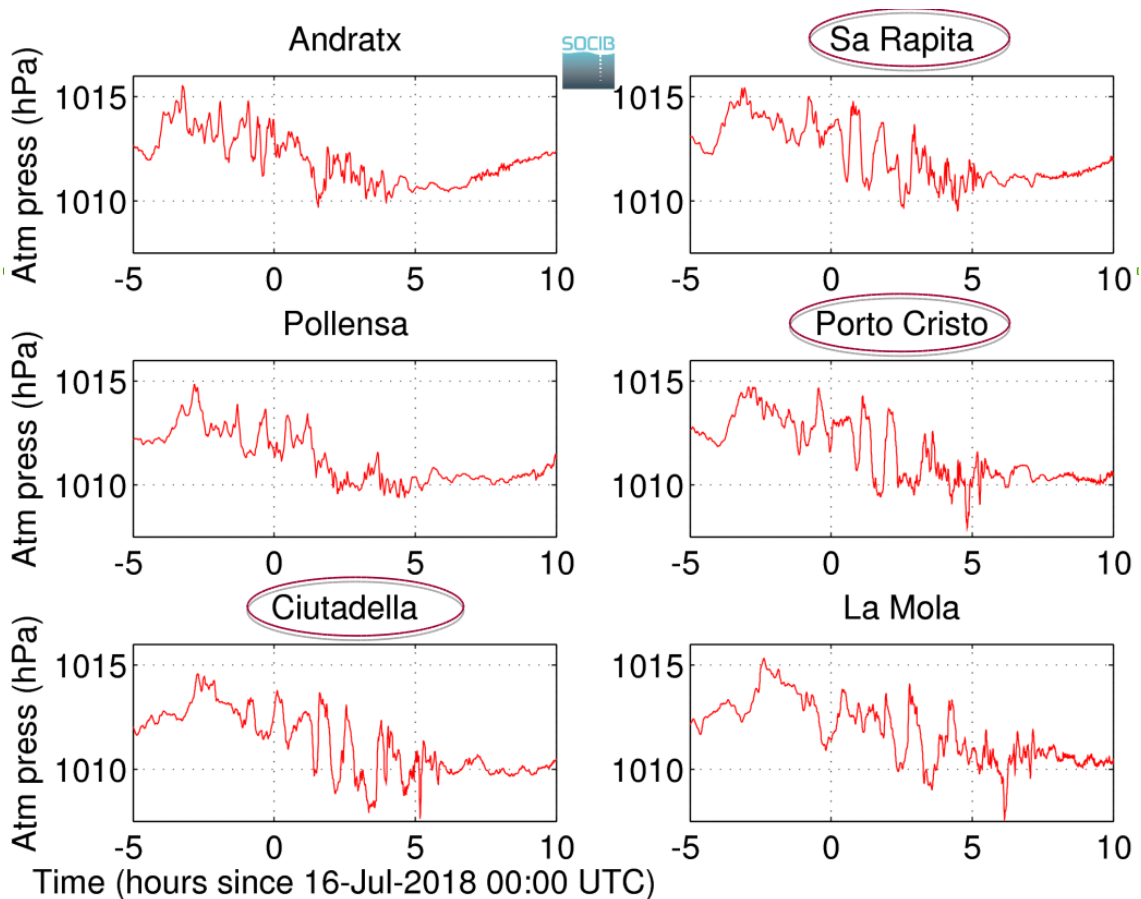


Figure 6: Observed sea level pressure time series at different stations.

As can be seen in figure 6, the time series of the three highlighted stations (Sa Rapita, Porto Cristo, Ciutadella) show very similar patterns. This shows a clear propagation of the atmospheric disturbance from the southeastern part of Mallorca towards Ciutadella.

ROMS was then forced by the sea level atmospheric pressure signal from the Ciutadella station, propagated using the observed speed and direction of propagation from Porto Cristo to Ciutadella. The direction of this propagation is known to be also fundamental in order to produce extreme events (*Licer et al., 2017*).

In Ciutadella, the sea level oscillation of the simulation done with the synthetic forcing with a 2-min frequency shows some reasonable agreement with the observations.

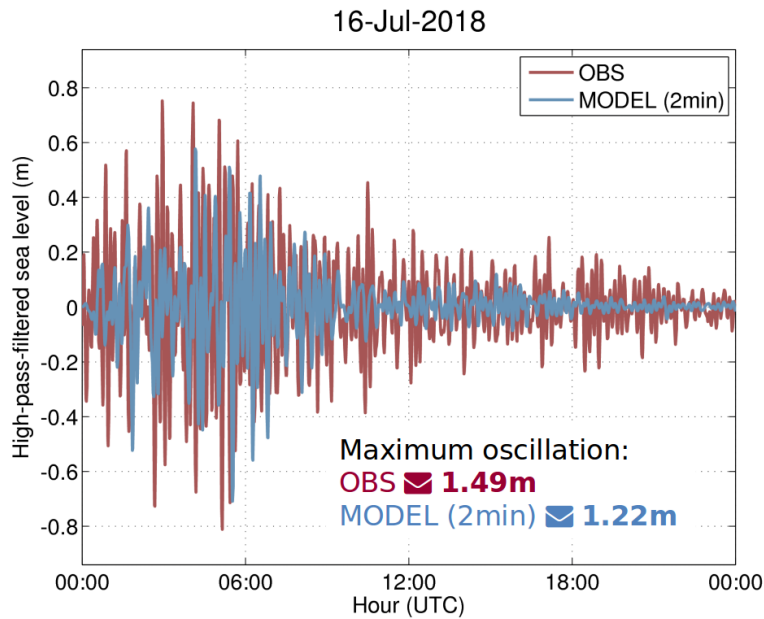


Figure 7: Comparison between sea level oscillations time series produced by the model (2 min forcing frequency) and observations at Ciutadella. Figure from *Gautreau (2018)*

However the response of ROMS is still slightly underestimated. Parallel experiments using 1 min and 30 sec forcing frequencies show that the temporal frequency is the origin of this underestimation. With 1 min forcing frequency, the modelled rissaga has a 1.46m amplitude which is a value very close to the 1.49m observed. With 30 sec forcing frequency, this reaches 1.48m

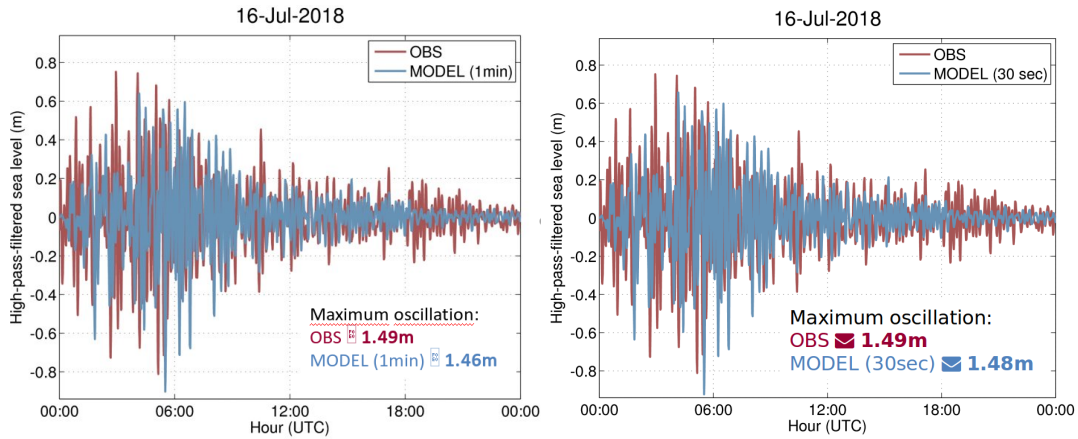


Figure 8: Same as Fig.7 but with a 1 min and 30 sec forcing frequencies. (a) Comparison between sea level oscillations time series produced by the model (1 min forcing frequency) and observations at Ciutadella (b) Comparison between sea level oscillations time series produced by the model (30 sec forcing frequency) and observations at Ciutadella. Figure from *Gautreau* (2018)

These experiments show that the oceanic model is able to properly reproduce the propagation of the atmospherically driven disturbance as well as the different amplification processes. This reveals that the main source of error in BRIFS predictions comes from the atmospheric model.

Another important result is that using outputs of the atmospheric model with a resolution of 2-min induces an underestimation of the final magnitude of the rissaga even with a realistic forcing. In spite of this, in this thesis the 2-min resolution is kept due to the increased computational cost associated with higher forcing frequencies.

2.3.3 WRF parameterizations

The sensitivity of the results to several parameterizations of WRF physics are investigated in this work. These parameterizations concern the planetary boundary layer, cumulus, microphysics, radiation, surface layer which are the most important parameterization of the physics in WRF (*Stergiou et al., 2017*). The election of these parameterizations is partly inspired from, the article of (*Horvath and Vilibić, 2014*) which studies the influence of cumulus and microphysics parameterizations. In this study, it was shown that the the model was very sensible to the convective parameterizations near the precipitation system. Also, it explains that the choice of the cumulus parameterizations may modulate the exact properties of the surface pressure oscillation which, at the end, triggered the meteotsunamis. As for the planetary boundary layer, the

study of *Renault et al.* (2011) shows that there is also a strong sensitivity in the atmospheric simulations results depending on the boundary layer scheme used. It defends that the different processes that occur in the planetary boundary layer play a crucial role in the determination of the sea level pressure intensity (variations around 20% to 40%).

The different schemes used in this thesis are described below as they are presented in the WRF manual

(http://www2.mmm.ucar.edu/wrf/users/docs/user_guide_V3.6/ARWUsersGuideV3.6.1.pdf).

Planetary Boundary Layer (PBL)

- **PBL1** *Mellor-Yamada Nakanishi and Niino* level 2.5 pbl. Predicts Subgrid turbulent kinetic energy terms.
- **PBL2** *Mellor-Yamada-Janjic* scheme. One dimensional prognostic turbulent kinetic energy scheme with local mixing
- **PBL5** *Yonsei-University* scheme. Non-local-k scheme with explicit entrainment layer and parabolic k-profile in unstable mixed layer

Cumulus Parameterizations (Cu)

- **Cu1** *Krain-Fritsch* scheme. Deep and shallow convection subgrid scheme using mass flux approach with downdrafts and CAPE removal time scale.
- **Cu6** *Tiedtke* scheme. Mass-flux type scheme with CAPE-removal time scale, shallow component and momentum transport.
- **Cu3** *Grell-Devenyi (G-D)* ensemble scheme. Multi-closure multi-parameter, ensemble method with typically 144 sub-grid members.

Microphysics (MP)

- **Mp6** *WRF Single-Moment 6-class* scheme. A scheme with ice, snow, and graupel processes suitable for high-resolution simulations.
- **Mp7** *Goddard* microphysics scheme. A scheme with ice, snow and graupel processes.

- **Mp8** New *Thompson* scheme. A new scheme with ice, snow, and graupel processes suitable for high resolution simulations. This adds rain number concentration.

Surface Layer (sfclay)

- **Sfclay1** *Revised MM5 surface layer* scheme. Remove limits and use update stability functions
- **Sfclay2** *Eta similarity*. Based on Monin-Obukhov with zilitinkevich thermal roughness length and standard similarity functions from look up tables.

Longwave radiation (ra lw)

- **Ra lw1** *RRTM* scheme. Rapid radiative transfer model. An accurate scheme using look up tables for efficiency. Accounts for multiple bands and microphysics species.
- **Ra lw4** *RRTMG* scheme. It includes MCICA method of random cloud overlap.

Shortwave radiation (ra sw)

- **Ra sw2** *Goddard shortwave* scheme. Two-stream multi-band scheme with ozone from climatology and cloud effects
- **Ra sw4** *RRTMG shortwave* scheme. Short wave scheme with MCICA method of random cloud overlap

3 Rissaga characterisation: past cases

In this section we analyze past events of rissagas to try to identify possible common characteristics. As it was described by *Jansà et al. (2007)*, the rapid pressure oscillations created by the meteorological disturbance, are triggered by some atmospheric gravity waves and/or convective jumps. The rissaga events are often associated with a typical synoptic state of the atmosphere. This typical state is characterised by a three layer structure *Jansà et al. (2007)*. The first layer is determined by a low level Mediterranean air, with a weak depression close to the surface. The second one is formed by warmer African air around 850hPa. An inversion layer separates the low level Mediterranean air from a warmer African air. Above the second layer, an unstable layer is found between the African air and the colder air above. This layer is generally marked by significant vertical wind shear. Strong horizontal gradients are known to be the cause of the generation of atmospheric gravity waves. Under these synoptic conditions, as the ones explained above, these atmospheric gravity waves are trapped and they maintain their shape, intensity and they are able to propagate long distances (*Sepić et al., 2015*). Under an overlying unstable layer, a critical level exists in which the wind speed can equal to the speed of these trapped gravity waves so that these waves can be trapped in a stable atmospheric layer adjacent to the ground. So, when these conditions are fulfilled, the atmospheric gravity waves can propagate and affect the surface level, which may then trigger the rissaga generation process.

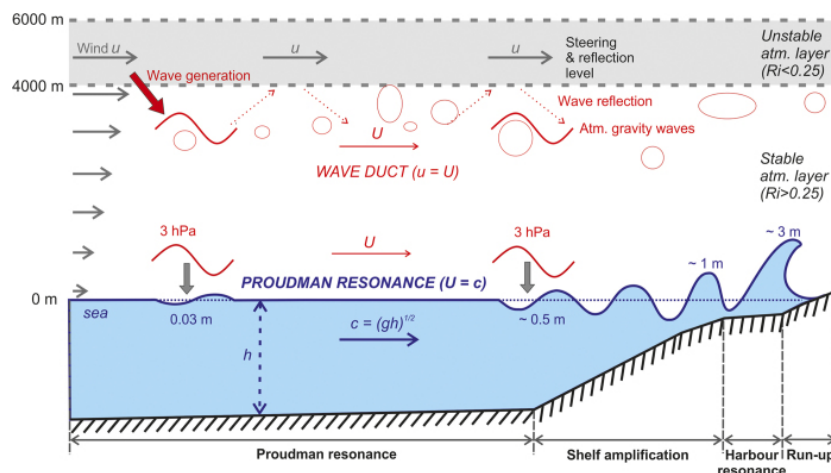


Figure 9: Generation and propagation of the trapped atmospheric gravity waves (duct waves), followed by the generation of long ocean waves which suffer the three different resonances explained in section 1.1.2. Figure from *Sepić et al. (2015)*.

As commented before, BRIFS simulations are available since 2014. The major rissaga events since 2014 have been compiled in the table in figure 10, also considering the major events of 15 June 2006 and 26 May 2008.

Date	Measured sea level oscillation (min-to-max)	Time (CET) of the rissaga
15-Jun-2006	(~4m ?)	20:50
26-May-2008	~1.65m	00:40
16-July-2018	1.49m	07:05
22-Apr-2015	1.49m	16:00
19-Aug-2014	1.45m	01:40
01-Aug-2015	1.35m	07:30 / 09:15
01-Apr-2016	1.24m	08:00

Figure 10: Major past events of rissaga. The colour indicates the level of warning and it depends on the magnitude of the rissaga. Data compiled by B.Mourre using SOCIB sea level gauge (except 2008 deduced from (Marcos *et al.*, 2009), and 2006 from eye witness).

In this thesis the seven largest events are studied. The 10-June-2018 case is also considered due to the exceptional magnitude of the prediction provided by BRIFS.

In all the cases a pressure time series will be first presented and then different images from satellite are described.

3.1 15-June-2006 (~ 4 m)

This first case has been largely studied since it was the largest rissaga from the last 30 years *Jansà et al.* (2007), *Montserrat et al.* (2006c), *Renault et al.* (2011), *Vilibic et al.* (2008)

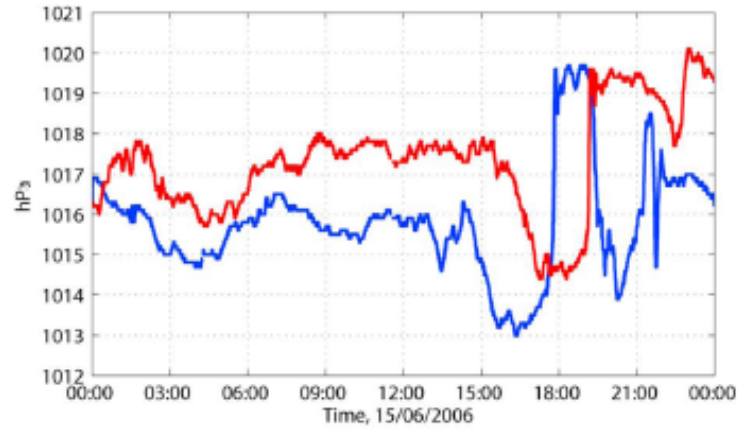
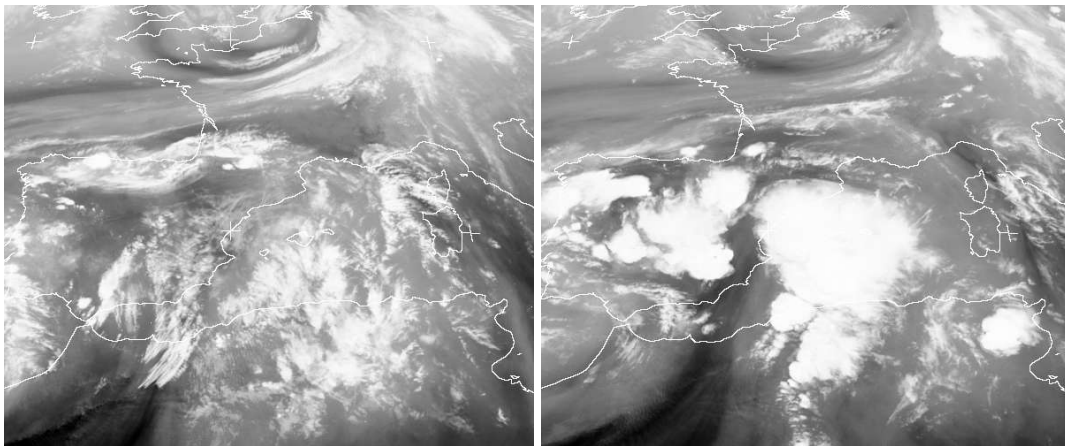


Figure 11: Pressure time serie for June 15, 2006. The blue line correspond to the observations in Palma while the red one corresponds to the observations in Mahón. (*Jansà et al., 2007*)

A pressure jump around 4hPa was observed at Mahon airport. This jump was produced by a convective nucleus that travelled along the Menorca channel beside a squall line with a velocity of 25 m/s (*Vilibic et al., 2008*).



(a) Mid-IR / Water Vapour channel at 1200UTC (b) Mid-IR / Water Vapour channel at 1800UTC

Figure 12: Images from Meteosat SEVIRI on June 15, 2006

Satellite images confirm the existence of the convective nucleus coming from the north of Africa.

3.2 25-May-2008 (~ 1.65 m)

The pressure time series were provided by Agustí Jansà.

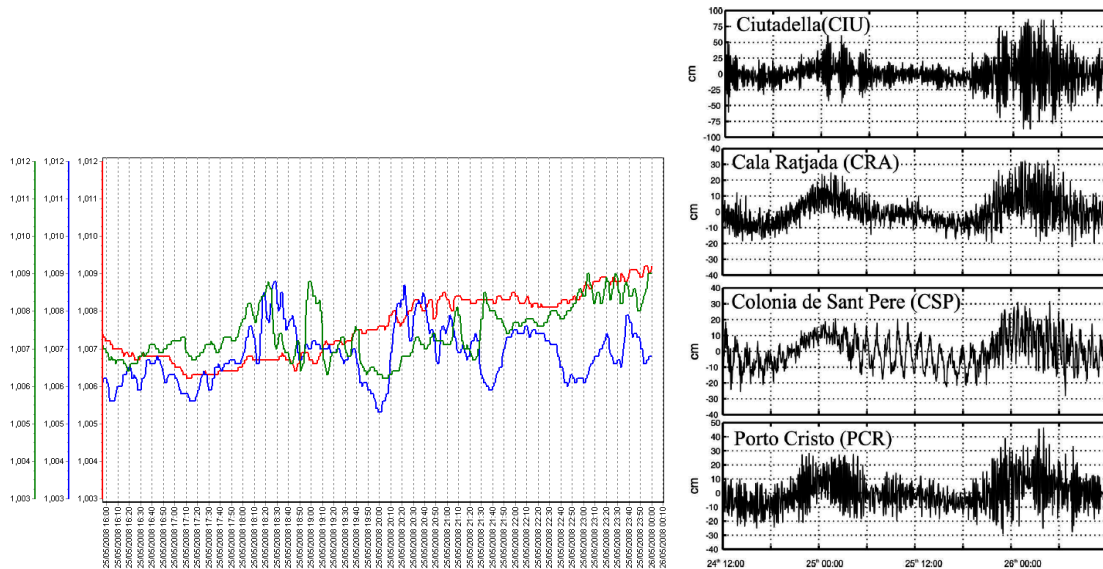
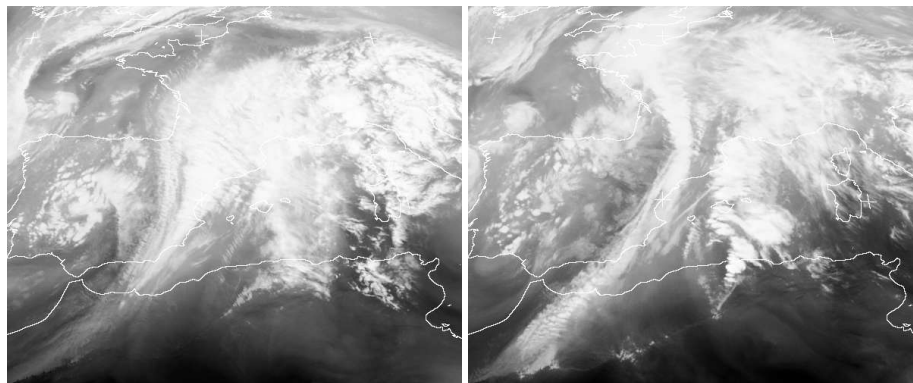


Figure 13: Pressure and sea level time series on May 25, 2008. (a) Pressure time series at different locations. Ibiza (red), Mallorca (green), Menorca (Ciutadella) (blue). (b) Sea level oscillations in different stations. (Marcos *et al.*, 2009)

The blue line corresponding to the time series in Menorca shows different atmospheric pressure with around 1.5 hPa magnitude that seem to indicate the presence of some atmospheric gravity waves. These oscillations start a few hours before the rissaga event.

Satellite images are introduced to confirm the presence of these gravity waves.



(a) Mid-IR / Water Vapour channel at 1200 (b) Mid-IR / Water Vapour channel at 1800

Figure 14: Images from Meteosat SEVIRI on May 25, 2008

It must be said that the rissaga occurred at 2240UTC and the images from figure 14 are taken at 1200UTC and 1800UTC. So these images next to the pressure time series confirm the presence of atmospheric gravity waves at least from 1800UTC. There are no evidences of any kind of convective phenomena neither in time series nor in satellite images . For this reason it

seems logic to think that the main features that caused this rissaga are the atmospheric gravity waves.

3.3 18-August-2014 (1.45 m)

This particular case has been studied in detail in *Jansà* (2014) and *Licer et al.* (2017).

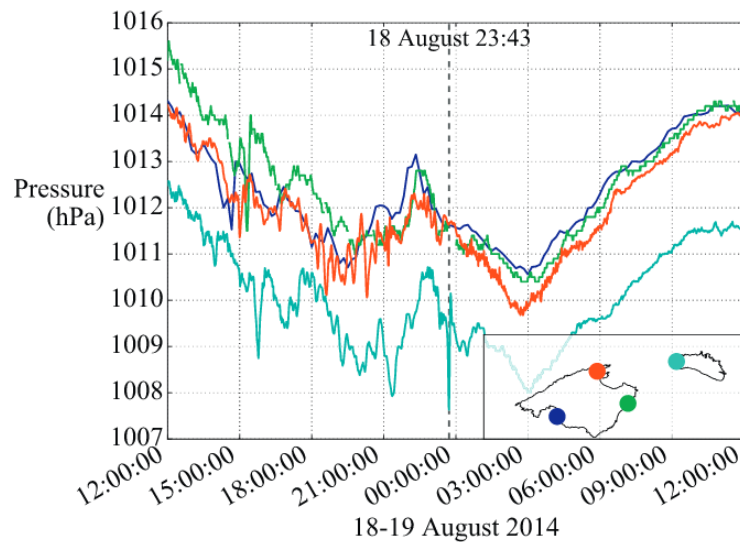


Figure 15: Pressure time series from different locations in the Balearic Islands for August 18, 2014. Figure from (*Licer et al.*, 2017)

The pressure time series shows a significant drop around 2hPa followed by a rise and then another drop. This pattern is typical when there is a presence of convective phenomena. In this case, it is a small convective nucleus (around 20 km) that has been formed over Mallorca and has travelled with a speed around 100 km/h (*Jansà*, 2014). The following satellite images corroborate the presence of this nucleus

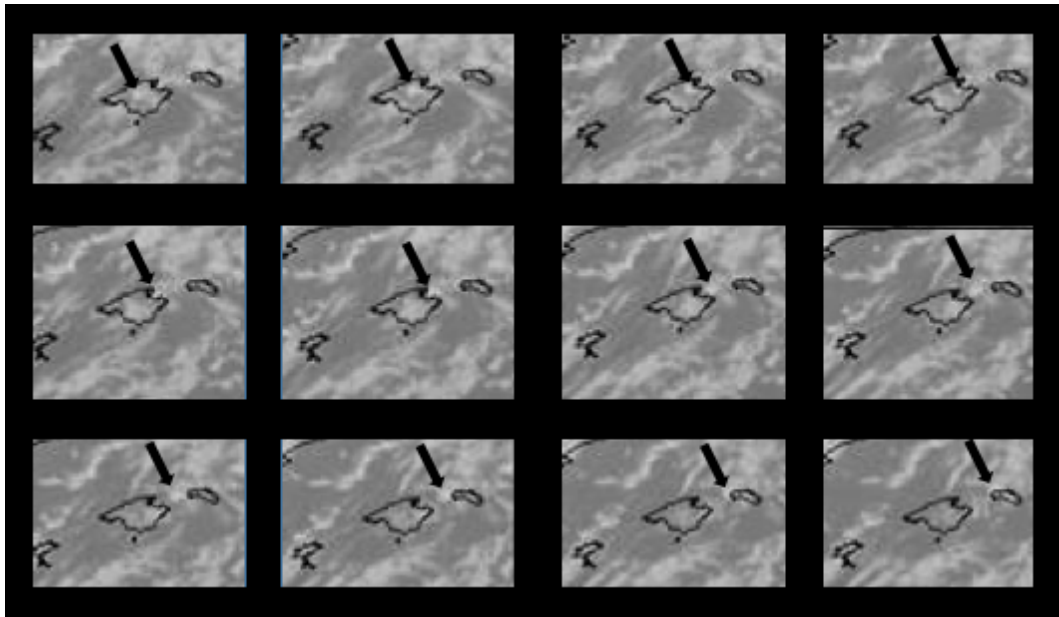


Figure 16: Images from Jansà, 2014. Pictures are taken every five minutes.

This nucleus was not detected in the pressure time series in Palma, Porto Cristo and Pollença. This particular case is rather unusual, but it shows that very small scale nucleus can also be at the origin of significant rissagues.

3.4 22-April-2015 (1.4 m)

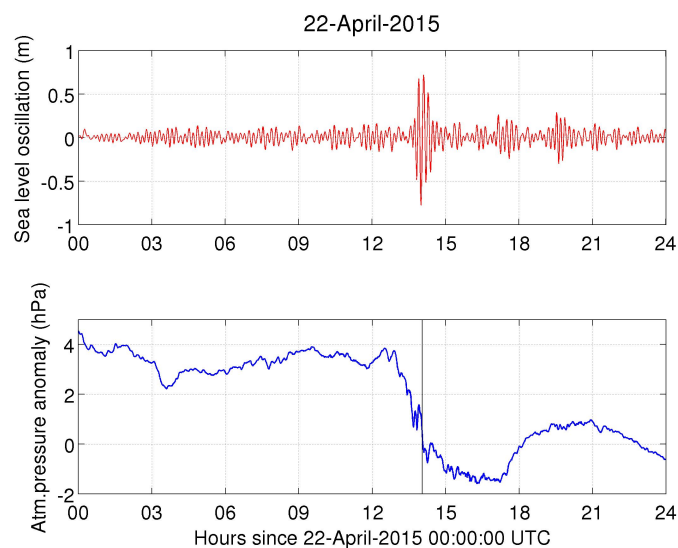


Figure 17: Pressure and sea level oscillations time series for April 22, 2015. Both images correspond to observations in Ciutadella inlet.

The pressure time series shows a marked drop of around 4 hPa in about one hour. This time period is too long to generate a strong response of the inlet (10.5 min resonance period). Associated with this drop are shorter oscillations, with one of these generating a sudden pressure drop around 1.5 hPa at the origin of the rissaga.

The sea level shows 3 or 4 significant oscillations, contrary to the 25 May 2008 case for instance when the harbour was oscillating significantly during several hours.

This calculation $p'(n) = p(n+1) - p(n)$ was applied to this series by A.Jansà.

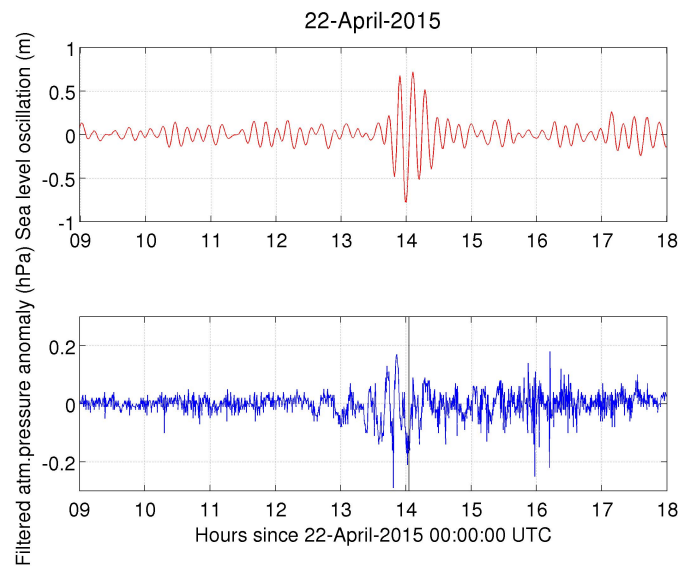
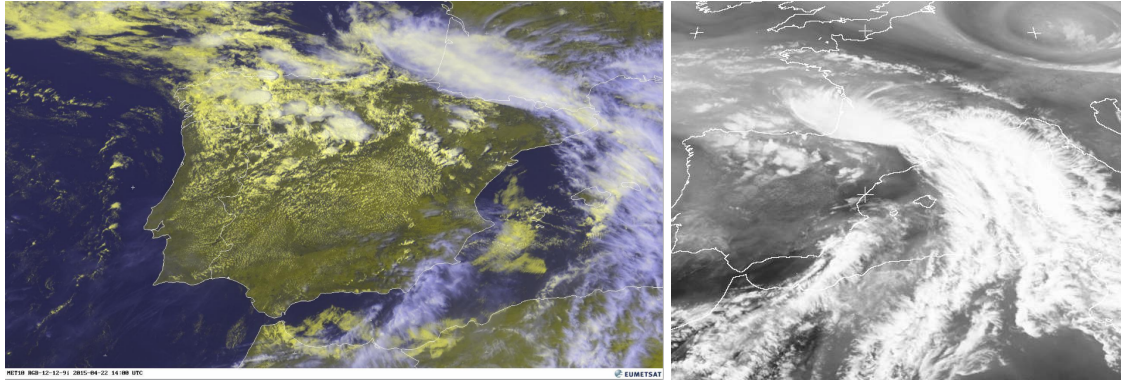


Figure 18: Same images as figure 17 but now the pressure time series shows the successive changes of pressure . This pressure time series was provided by Agustí Jansà.

The time series reveals the presence of atmospheric gravity waves. These waves started a few hours before the largest oscillation. The existence of these waves can also be seen in the images from the satellite.



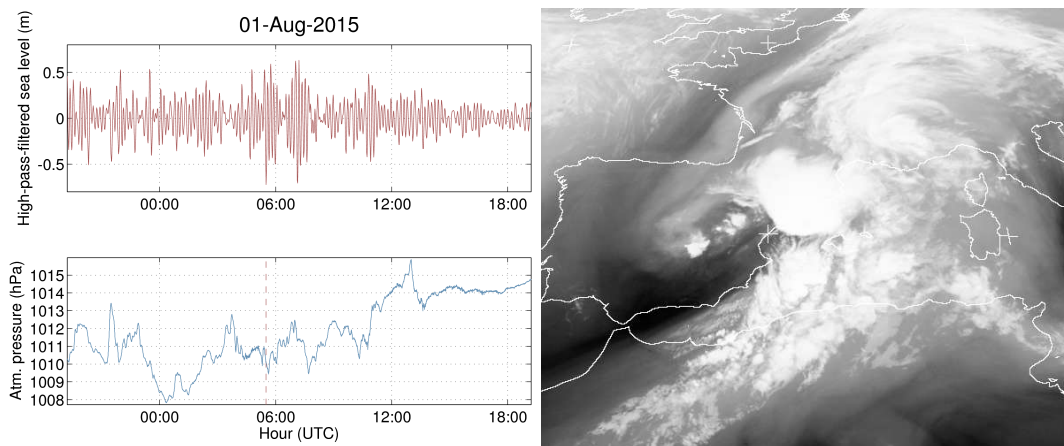
(a) Visible channel at 1400UTC

(b) Mid-IR / Water Vapour channel at 1500UTC

Figure 19: Images from Meteosat SEVIRI on May 25, 2008

In 19 (a) it is possible to see the streaked pattern in the clouds typical when there is presence of the atmospheric gravity waves. The figure also shows the direction of the propagation of this waves.

3.5 01-August-2015 (1.35 m)



(a) Pressure and sea level oscillations time series. (b) Mid-IR / Water Vapour channel at 0000UTC
Both images correspond to observations in Ciutadella inlet.

Figure 20: Observations for August 01, 2015.

While the pressure time series shows some small scale oscillations of moderate magnitudes (around 1-2hPa), the sea level was found to oscillate with large amplitudes during around 3 hours. The largest oscillation corresponds to a pressure drop of 1.5 hPa in around 15 min.

The satellite image shows a clear propagation coming from the north of Africa, together with the typical gravity waves stripes.

3.6 01-April-2016 (1.24 m)

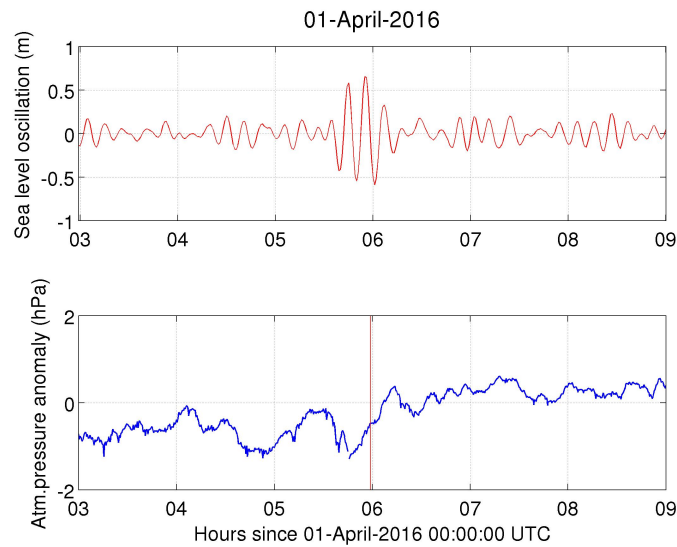


Figure 21: Pressure and sea level oscillations time series for April 01, 2016. Both images correspond to observations in Ciutadella inlet.

The pressure time series shows some oscillations of the order of 1hPa. The sea level oscillates with a magnitude less than 50 cm during a few hours before the main rissaga, which is characterised by 3 large oscillations of the harbour.

Fig 21 seems to indicate that some hours before the rissaga a gravity wave train passed over Menorca, but at the time of the rissaga there is a rise of the pressure that may indicate the presence of convective phenomena.

Satellite images support the existence of the gravity waves train hours before the main event, but do not clarify the existence of the convection phenomena. This aspect is difficult to distinguish due to different tones in the reflectivity. For this reason taking a look into radar images could provide additional information.

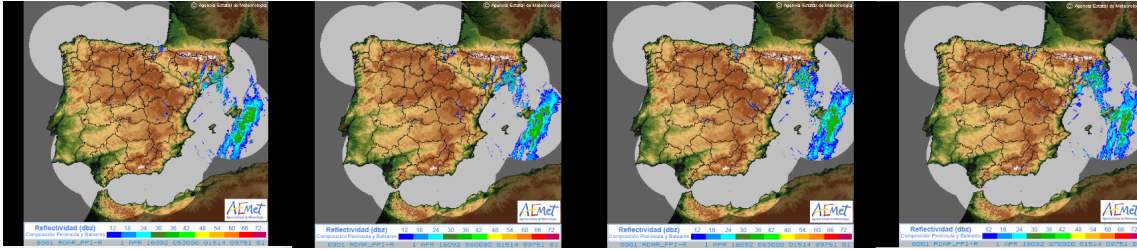


Figure 23: Radar images from the AEMET for this case. Images from 0530UTC to 0700UTC every images is taken every 30 min.

With these four images it is not possible to confirm the existence of a strong convection phenomena. It is true that they show rain episodes, but they do not show any kind of typical convective structure. Although these do not rule out the possibility that these convective phenomena exist.

3.7 16-July-2018 (1.49 m)

This case was already introduced in the previous section (2.3.2). It is also a clear case of gravity waves. Here the pressure time series alongside with the sea level oscillation time series is presented.

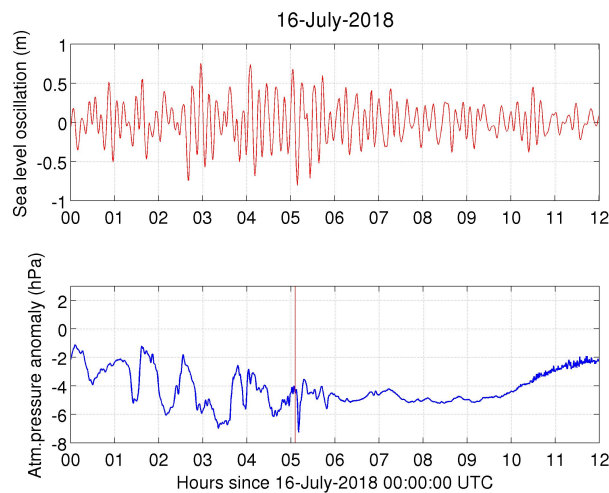
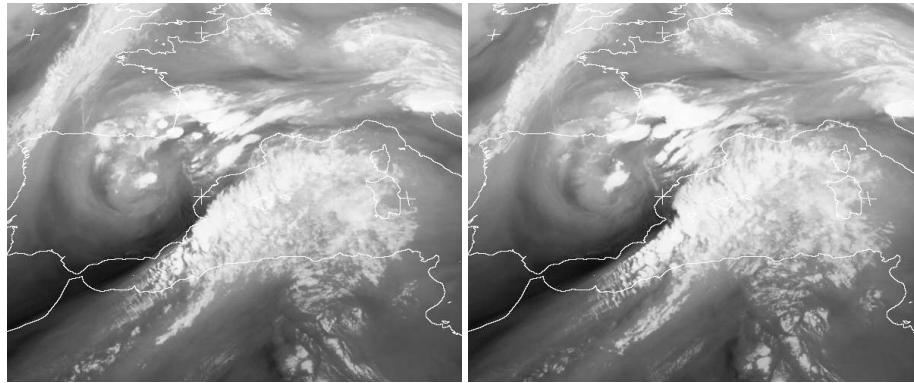


Figure 24: Pressure and sea level oscillations time series for July 16, 2018. Both images correspond to observations in Ciutadella inlet.

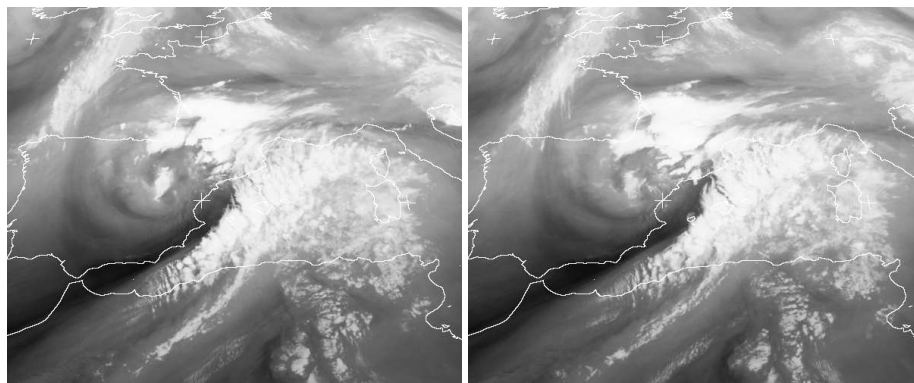
As in most of the previous cases, the main cause of the rissaga are the atmospheric gravity waves. The barometer in Ciutadella had been recording oscillations with an amplitude around

4hPa for a few hours. Moreover, the largest oscillation seems to be linked to a convective signal with a short drop of atmospheric pressure of around 3hPa, similar to what was observed for the case 18 August 2014.

These gravity waves can be seen in the satellite images.



(a) Mid-IR / Water Vapour channel at 0200UTC (b) Mid-IR / Water Vapour channel at 0300UTC



(c) Mid-IR / Water Vapour channel at 0400UTC (d) Mid-IR / Water Vapour channel at 0500UTC

Figure 25: Images from Meteosat SEVIRI on July 16, 2018

Here a clear propagation is detected from the north Africa.

3.8 Synthesis

In this section, the main objective was to characterise and understand the seven cases of the main rissagas of the last years. These were generated by squall lines, gravity waves and convective processes. The sea level oscillation was also found to have different duration, from around half an hour to several hours. This characterisation also demonstrates that the small-scale processes

and details of the perturbations have a crucial role in the generation of the rissagas. These small pressure disturbances have a stochastic character that makes the prediction fundamentally very challenging. This also probably points out the necessity to move towards ensemble forecasting.

This is the topic of the next section, which investigates BRIFS ensemble simulations through the performance of WRF sensitivity experiments.

4 WRF sensitivity experiments

Let's first introduce the results of the deterministic predictions provided by BRIFS for these past major events of rissaga. These simulations were run using the WRF 3.3.1 version.

Date	Measured sea level oscillation (min-to-max)	BRIFS prediction (sea level oscillation)	Time (CET) of the rissaga	BRIFS prediction (rissaga time CET)
15-Jun-2006	(~4m ?)	3.10m <small>hindcast</small>	20:50	22:25
26-May-2008	~1.65m	1.16m <small>hindcast</small>	00:40	01:00
16-July-2018	1.49m	0.87m	07:05	04:50
22-Apr-2015	1.49m	0.66m <small>hindcast</small>	16:00	18:20
19-Aug-2014	1.45m	1.11m <small>hindcast</small>	01:40	20:30 (18-Aug)
01-Aug-2015	1.35m	1.00m	07:30 / 09:15	07:20
01-Apr-2016	1.24m	0.51m	08:00	12:40

Figure 26: Major rissaga past events, now including BRIFS prediction. The colours of the alert are the same as before (table compiled by B.Mourre).

The table shows that the model was able to represent some significant signal (>50cm) in all these cases, but systematically underestimated the actual magnitude of the phenomena. It generated rissagas > 1m in four of the seven cases, and was able to generate an extreme oscillation (>3m) for the case of 15 June 2006.

In order to better understand the behaviour of the model, ensemble simulations have been performed for these different cases so as to investigate the sensitivity of this problem to the physical parameterizations. To visualise all the simulations, the following table is introduced. Notice that some values may differ between figure 26 and the next figures since the sensitivity experiments were simulated using the WRF 3.6.1 version due to a recent update of the system.

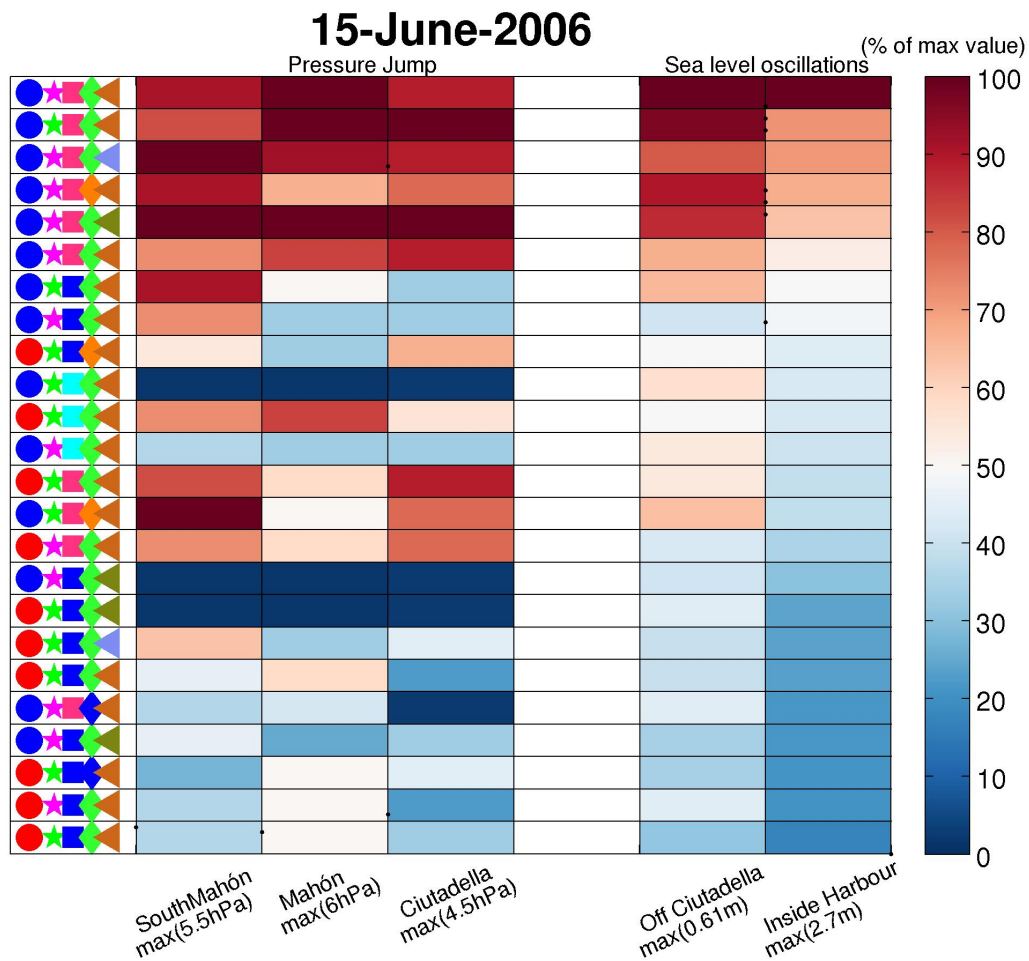


Figure 27: BRIFS simulation for the June 15, 2006 case. Every row corresponds to one simulation.

The symbols in figure 28 indicate the physical parameterizations used in the simulation. The legend of these symbols can be found in the following table.

Radiation		Radiation dt		PBL			Cumulus			Microphysics		
1-2	4	4	10	1	2	5	3	1	6	8	7	6
●	●	★	★	■	■	■	◆	◆	◆	◀	◀	◀

Figure 28: This legend represents every parameterization used in the different simulations. Every form corresponds to a different type of parameterization and every colour represents different schemes. These schemes are described in 2.3.3.

Now, the colour of each grid corresponds to the percentage with respect the maximum value across the simulations. This maximum value is indicated in the bottom axis. The first three columns represent the pressure jump in different points. The simulations are ranked according

to the magnitude of the rissaga in Ciutadella. The other two are the sea level oscillations inside and outside Ciutadella inlet. For instance, in the third column, the maximum jump is obtained for the simulation 5 with a 4,5 hPa jump, providing a 100%.

This table points out several interesting results both for the study of this particular case, and for the general prediction of rissagas.

The main objective of this figure for the study of this rissaga is to see the correlation between the existence of the pressure jump in Ciutadella and the final rissaga. It is clear that in order to produce a rissaga, a pressure jump is necessary. However, a significant rissaga is not generated in every simulation where the pressure jump exists. The main reason is that apart from the existence of the pressure jump, this final rissaga is sensitive to the period associated with this pressure jump. As an important outcome, this table shows the high sensitivity of the results to the physical parameterizations of the WRF model. This opens the possibility to create ensemble of simulations in order to make probabilistic predictions instead of deterministic predictions.

Due to its computational cost, the table in fig.4 is reduced to a nine member ensemble in order to be able to study the different cases presented in section 3

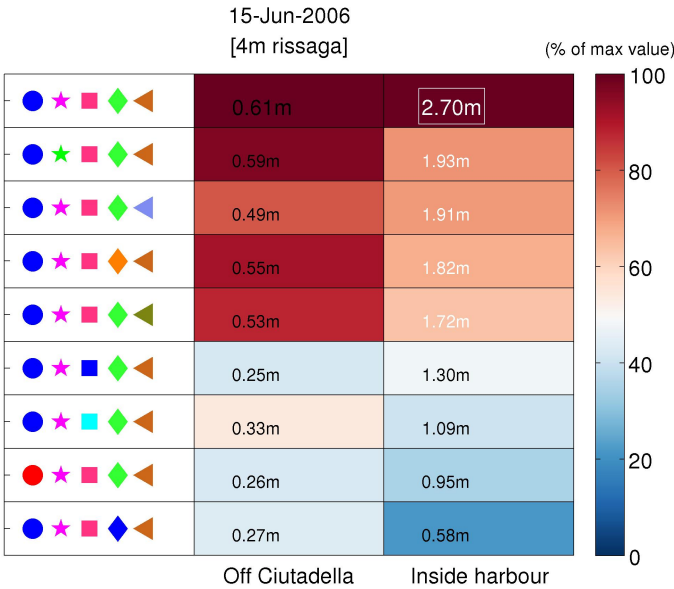


Figure 29: The reduced ensemble. Nine simulations make up this ensemble to study the seven different cases.

This table is a bit different form the previous one in that only the sea level oscillations inside

and outside Ciutadella harbour are represented. The value of the maximum sea level oscillations are indicated in every cell. In the Inside harbour column, the value which is highlighted with a rectangle, indicates the result most similar to the observations.

4.1 Toward the ensemble prediction

The table presented before starts to give some clues toward the creation of an ensemble, in order to improve the predictions. There is also another particularly interesting case where the BRIFS predictions significantly overestimates the rissaga magnitude.

This case is one of the few cases of overestimation. The observations of April 22, 2015 recorded a 0.63 m rissaga while the BRIFS prediction was 2.85 m. This is quite a surprising result, especially when the model usually underestimates the rissaga value. So the same nine simulations done for June 15, 2006 case were also run for this case.

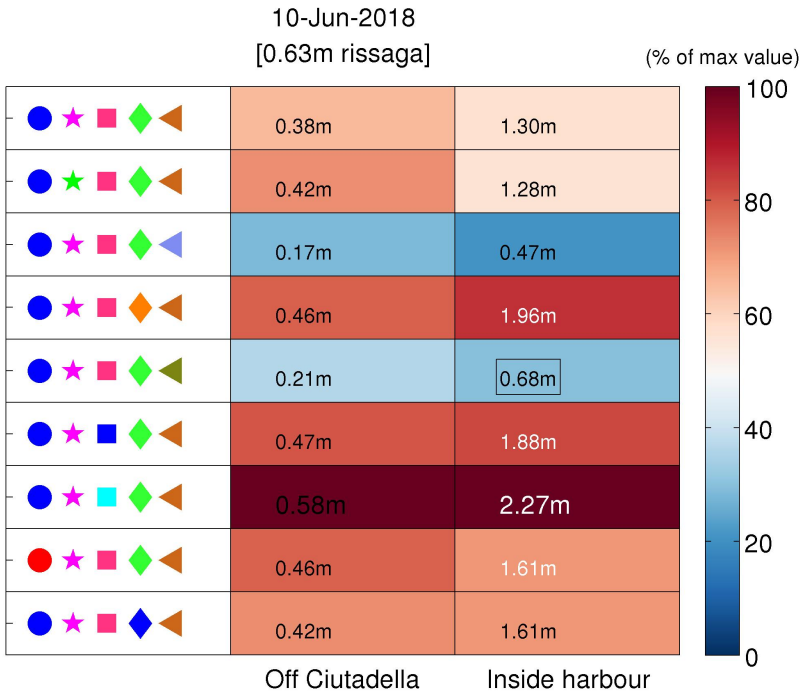


Figure 30: Ensemble simulation results for 10-June-2018.

Here the large range of values is exposed. It goes from 0.68m to 2.27m. This figure confirms the strong sensitivity of the results to the physical parameterizations. So if only one simulation is done in order to predict the future rissaga, it could happen that this simulation provides an extreme value. With a deterministic prediction, a "random" factor is likely to significantly affect

the final result. This randomness is a limitation for deterministic operational predictions, and points out the need for ensemble predictions. To further evaluate the potential of ensemble predictions, the same ensemble has been simulated for the seven most important cases of rissaga.



Figure 31: Ensemble simulations result for every case studied in this thesis.

Figure 31 confirms the variability of these results to the different physics parameterizations. A wide range in the sea level oscillation can be observed in every case due to this variability. Also it seems that there is no parameterization that performs better than another one. One can not identify a single parameterization that constantly simulated the best value in comparison to the observations (the one highlighted with the rectangle). It is true that the same simulation reproduces the maximum value of the rissaga in some cases but then it is completely different in the others. Analogously this variability occurs with the minimum and the best value. However, the most important result is probably that in all cases except April 22, 2015 the range of the ensemble covers the observations. It is easier to see this result in the following scatter plot.

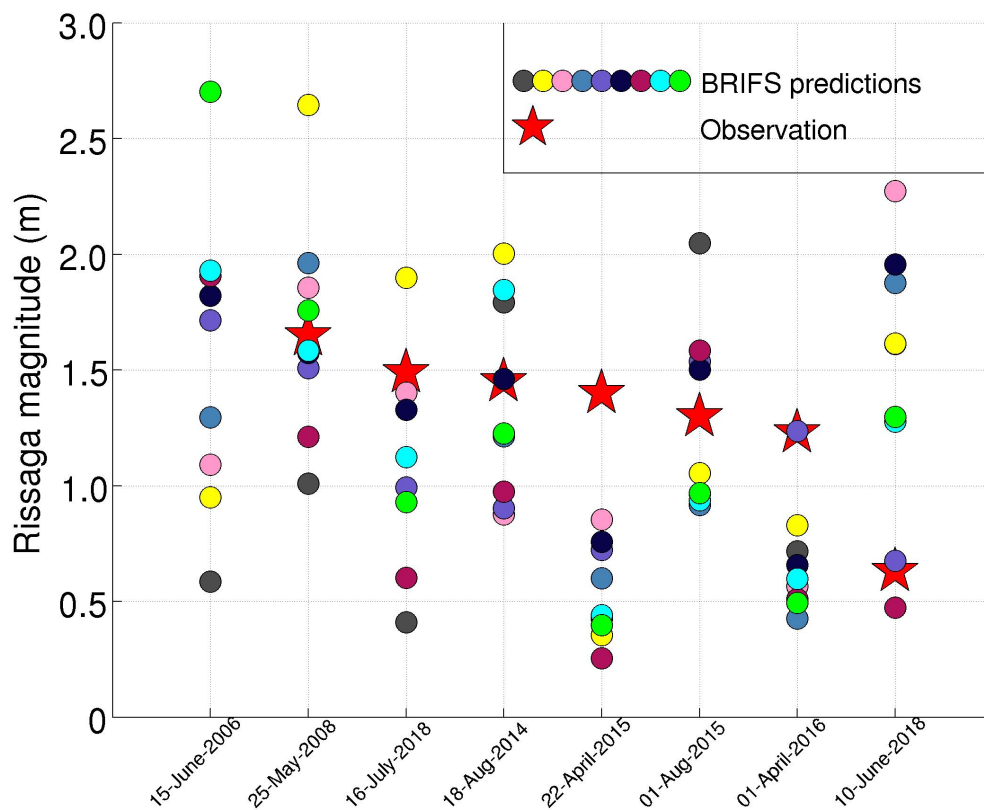


Figure 32: Ensemble range for every case.

4.2 Model ensemble evaluation

In this section the main idea is to evaluate the model ensemble simulations in order to see if the main features that were identified in the previous section 3 are represented. From all the cases explained earlier three rissagas cases can be distinguished in terms of features. The way in which the model will be evaluated will be by comparing the main features observed in the minimum, maximum and best case from the corresponding ensemble.

4.2.1 June 15, 2006

The first case that is evaluated is that of June 15, 2006. The reason is because in this case a clear squall line travels with the pressure jump. This convective phenomenon together with the gravity waves triggered the biggest rissaga over the last twenty years. The most important thing that the model should reproduce is the pressure jump and the squall line travelling through the Menorca channel. To study this, some snapshots of the mean sea level pressure are first introduced. They show if the model reproduces the squall line, its location and its intensity. The pressure time series are also presented. It will give information about the pressure jump, its magnitude, its period, etc

Let's start showing the snapshots from the maximum, minimum and best case.

Maximum and best simulation:

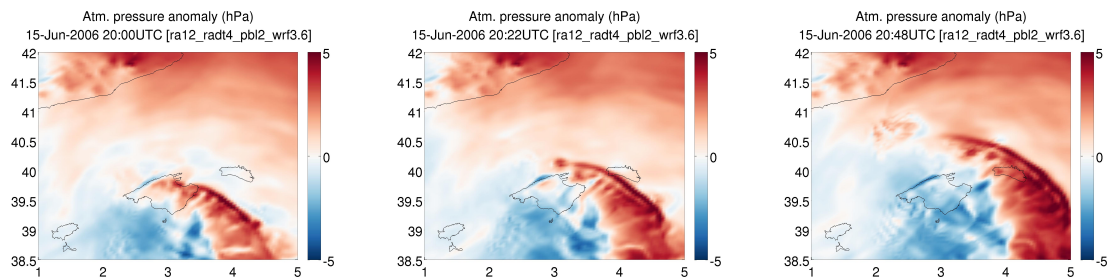


Figure 33: Simulation of the best and maximum case for June 15, 2006. In this particular case, the maximum and the best coincide.

Minimum simulation:

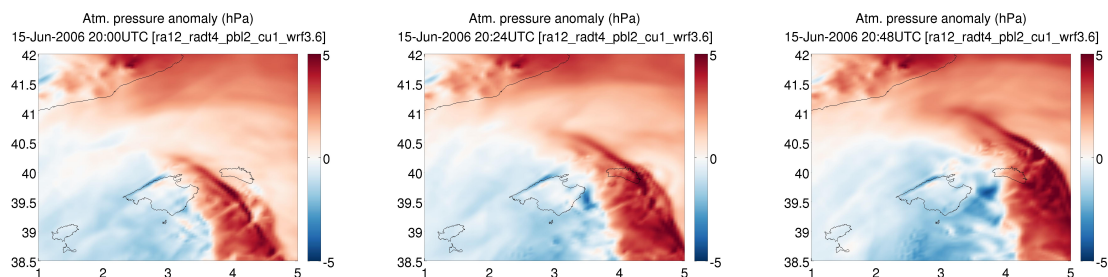


Figure 34: Simulation of the minimum case for June 15, 2006.

Surprisingly in both cases it seems that a squall line is formed. The model is able to reproduce the squall line in all the range of the ensemble even in the minimum case.

So, knowing that the model is able to reproduce this squall line, lets see how the pressure time series is represented.

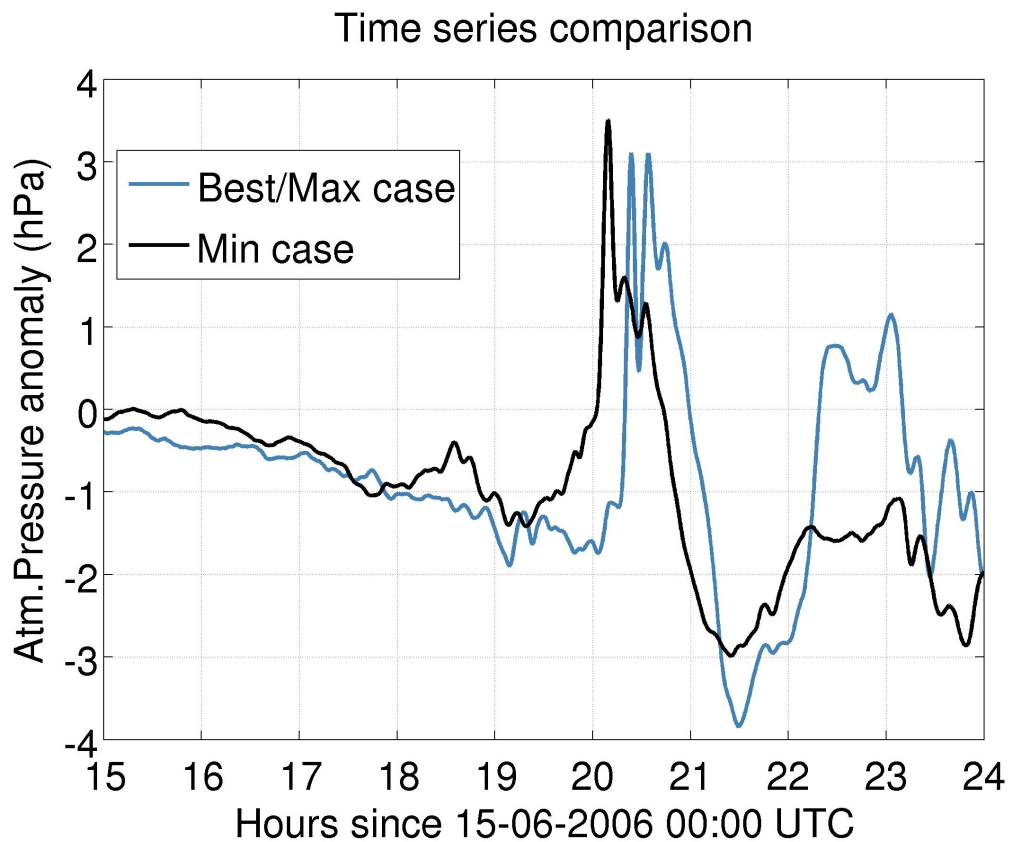


Figure 35: Time series comparison between the different simulations at Ciutadella's inlet.

Both time series are quite similar, showing a significant pressure jump. The difference is very probably related to the oscillations that occur after the pressure jump. In the max and best simulation this oscillation seems to have bigger magnitude than the min simulation. Also, the period of the pressure jump from the best/max simulation is closer to the fundamental period than the min simulation. This is a crucial factor in order to produce extreme rissaga events.

4.2.2 August 18, 2014

As it was explained in 3.3 this is another singular case . The small convective cell that produced the meteotsunami travelled along the channel with the exact speed and direction. Now let's see if the model is able to reproduce this convective phenomenon.

Max case

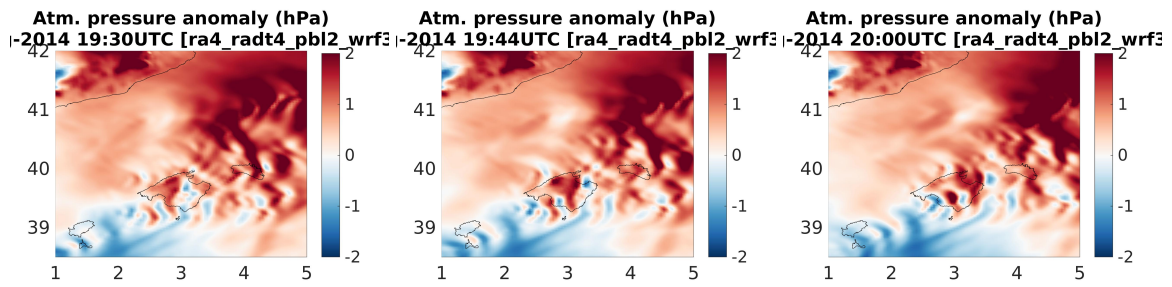


Figure 36: Simulation of the maximum case for August 18, 2014. Mean sea level pressure snapshots.

Min case

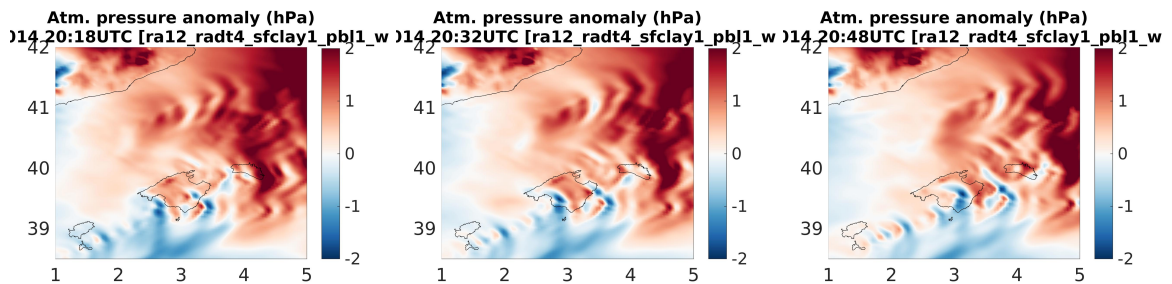


Figure 37: Simulation of the minimum case for August 18, 2014. Mean sea level pressure snapshots.

Best case

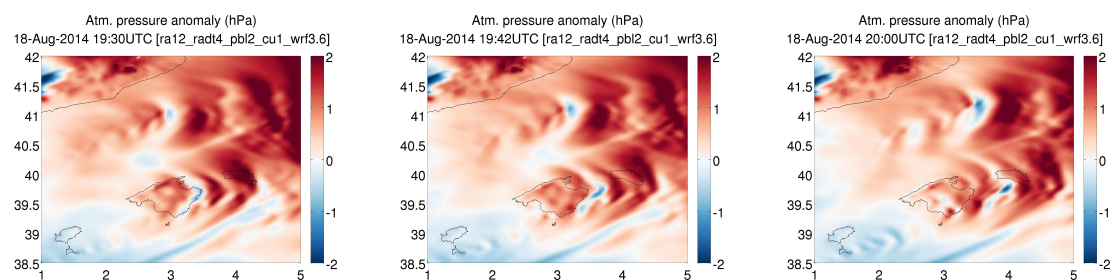


Figure 38: Simulation of the minimum case for August 18, 2014. Mean sea level pressure snapshots.

A convective phenomena seems to appear in these mean sea level pressure figures. It is bigger than the one observed in the satellite images but the pattern of jump, drop and jump seems to exist. It also has the right direction. It is difficult to see the difference between the maximum and best simulations in these figures, but in the minimum simulation it seems that the

convective phenomena is weaker in intensity. So maybe the time series gives more clues about the differences between each simulation.

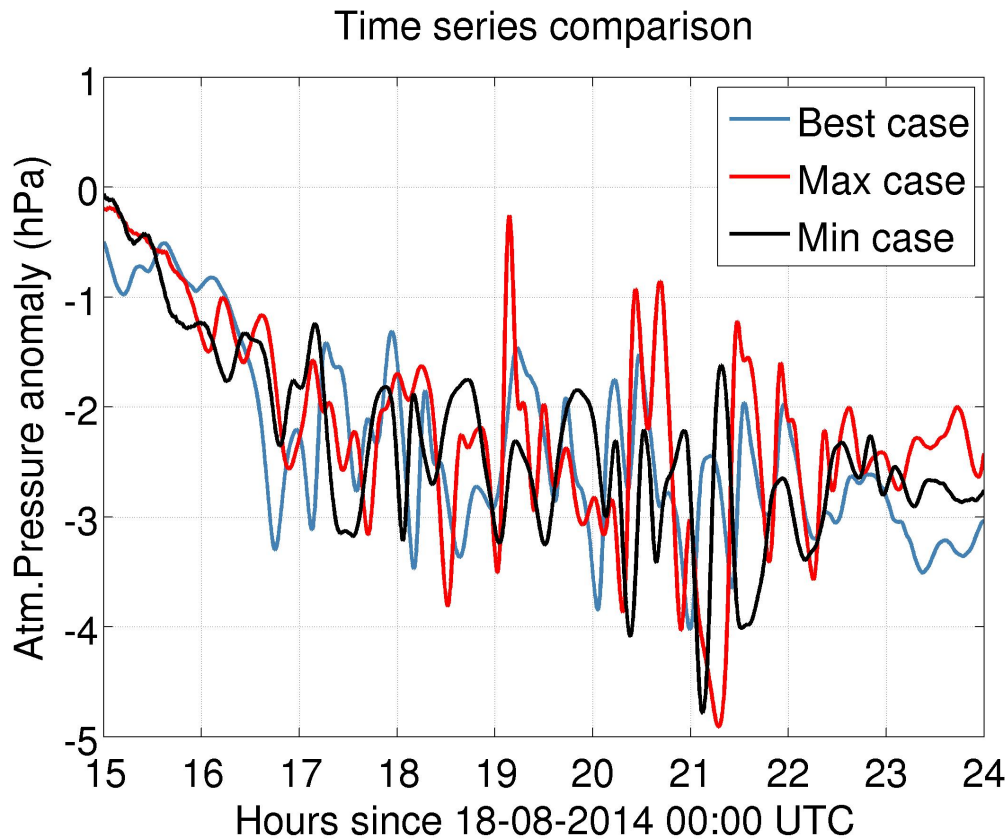


Figure 39: Pressure time series comparison between the different simulations at Ciutadella's inlet.

Here the time series show a great variability in all the simulations. If the time when the rissaga occurs is checked, some differences can be observed in the maximum and best simulations. The max case occurs at 1930UTC while the best simulation occur at 20:00UTC. In the simulation leading to the maximum rissaga, a huge drop is found followed by a little jump. At the same time, the drop in the best simulation is smaller compared to the maximum simulation. On the contrary, the pressure jump is bigger in the best simulation than the jump in the maximum simulation.

4.2.3 July 16, 2018

The last case of study shows the presence of gravity waves. The MSLP snapshots are introduced in order to check if the model reproduces this phenomenon.

Max case

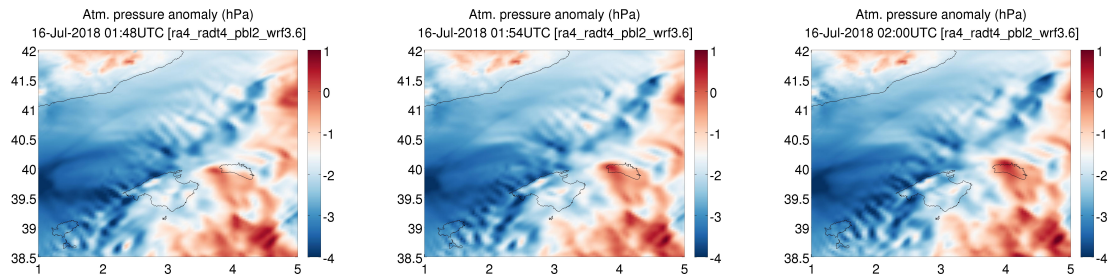


Figure 40: Simulation of the maximum case for July 16, 2018. Mean sea level pressure snapshots.

Best case

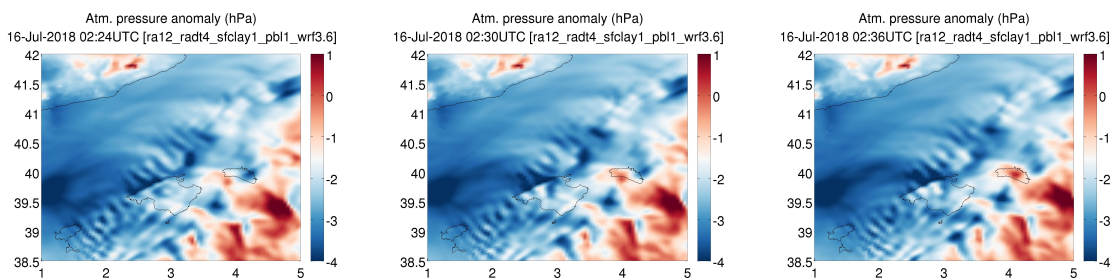


Figure 41: Simulation of the best case for July 16, 2018. Mean sea level pressure snapshots.

There are clear evidences of the presence of the waves in both maximum and best simulation. However the characteristic pattern is not situated over the Menorca channel, it is displaced to the north of Mallorca. Another element that can be seen: a convection phenomenon is moving toward Menorca from the channel. It seems to be a convective phenomenon. So taking into account that there are evidence of the presence of gravity waves, this convective phenomenon may be produced by this waves. The pressure time series are introduced.

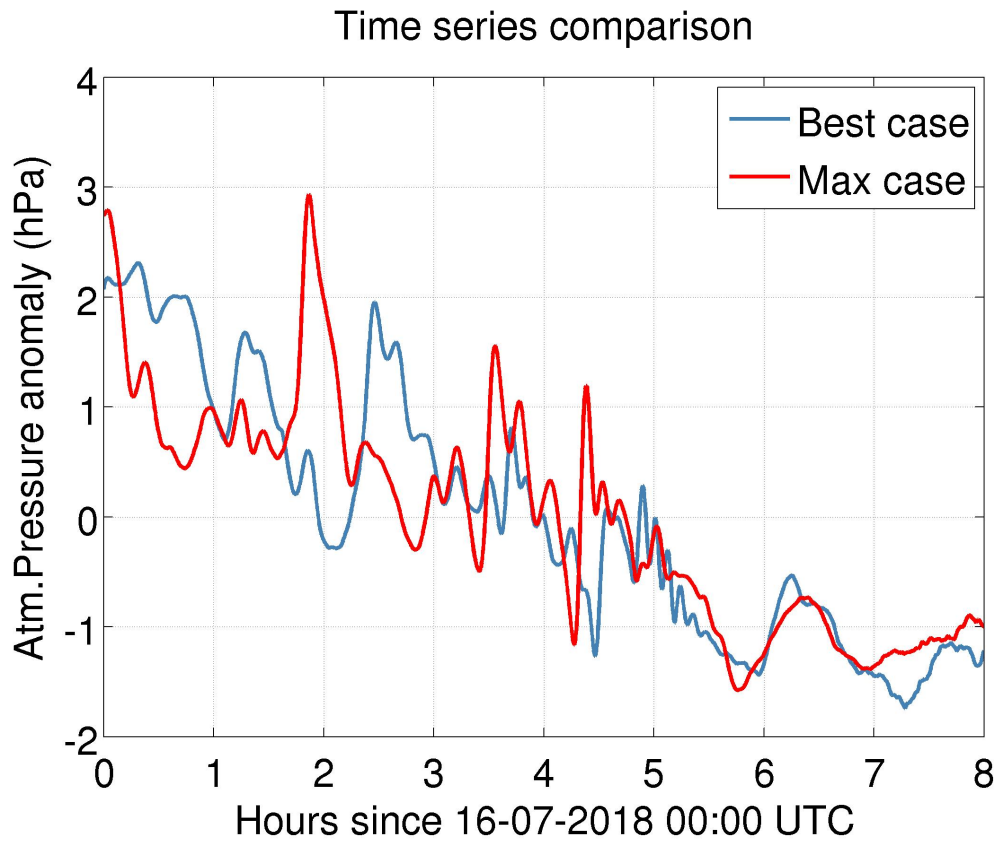


Figure 42: Pressure time series comparison between the different simulations at Ciutadella's inlet.

These time series confirm the possibility of this convective phenomena. In both simulations a pressure jump is detected. This jump is higher in the maximum simulation than in the best simulation. So this may be the reason of the difference between each simulations. Once this element has passed over Menorca, the signal of the gravity waves appears in Ciutadella.

5 Conclusions

The main goal of this thesis has been to understand the behaviour of the BRIFS system so as to improve the way the rissagas are predicted using a full atmospheric-ocean modelling system, providing support to the official AEMET warning system.

The first part of the thesis has studied and characterised the seven largest rissagas of the last years. All rissagas studied have passed the 1 m height. In this characterisation three different types of rissaga have been detected. Usually they are produced by the presence of some atmospheric gravity wave. This was not the case in 2 occasions. The June 15, 2006, apart from the existence of these atmospheric gravity waves, there was also a strong convective phenomena called squall line accompanied with a strong jump in pressure. And for the August 18, 2014 the rissaga was produced by a small convective cell that travelled through the Menorca channel right into Ciutadella's inlet.

Provided a previous validation of the ROMS model, this thesis has been focused on the improvement of the atmospheric component of the BRIFS system. The main objective was to investigate the sensitivity of the WRF model to different parameterizations. Two experiments were performed as motivation to evolve through an ensemble prediction. They showed a great sensitivity to the physical parameterizations of the model. This is a strong evidence of the randomness of the phenomenon, which constitutes a limitation of the deterministic forecast system.

The creation and evaluation of ensembles of predictions shows that in all cases except the April 22, 2015, the ensemble covers a range that includes the observations . It also reproduces the main features that characterised every case. This result demonstrates the potential of ensemble predictions of the BRIFS system.

6 Future work

There is some work that has not been done in this thesis due to lack of time. More simulations for the April 22, 2015 are needed. It is the only case for which the range of the ensemble does not embrace the observation.

This study has only considered the sensitivity to the WRF physical parameterizations. The effect of the initial conditions should be considered in the future.

For the case of July 16, 2018 the rissaga did not only happen in Menorca. There were also significant rissagas in other locations such as Andratx and Alcúdia. The reason of these rissagas is unknown so it must be studied.

A major challenge now consists in optimising computing costs so as to be able to implement the ensemble forecasting system in an operational way.

Alternatively, another approach could be developing a machine learning algorithm which decides which parameterization should be used as function of the atmospheric state. A large data base could be built considering all past cases and a machine learning algorithm could “choose” the optimal parameterization for the present case.

In the University of the Balearic Islands there is another rissaga prediction method. The main objective of this method is to capture the physical processes that leads to the generation of the rissaga with low computational cost. It uses a model created by

References

- Gautreau, L. (2018), Modelling and prediction of meteotsunamis affecting Ciutadella harbour, Menorca , SOCIB Modelling and Forecasting internal report.
- Green, E. G. (1838), On the Motion of Waves in a variable Canal of small Depth and Width, *Transactions of the Cambridge Philosophical Society*, 6, 457.
- Horvath, K., and I. Vilibić (2014), Atmospheric mesoscale conditions during the Boothbay meteotsunami: a numerical sensitivity study using a high-resolution mesoscale model, *Natural Hazards*, 74(1), 55–74, doi:10.1007/s11069-014-1055-1.
- Jansà (2014), Rissagues: El caso de 19 de Agosto 2014, *Asociación meteorológica española. Tiempo y clima*, (46), 43–48.
- Jansà, A., S. Monserrat, and D. Gomis (2007), The rissaga of 15 June 2006 in Ciutadella (Menorca), a meteorological tsunami, *Advances in Geosciences*, 12, 1–4, doi:10.5194/adgeo-12-1-2007.
- Licer, M., B. Mourre, C. Troupin, A. Kriemeyer, A. Jansá, and J. Tintoré (2017), Numerical study of Balearic meteotsunami generation and propagation under synthetic gravity wave forcing, *Ocean Modelling*, 111(6), 38–45, doi:10.1016/j.ocemod.2017.02.001.
- Marcos, M., S. Monserrat, R. Medina, A. Orfila, and M. Olabarrieta (2009), External forcing of meteorological tsunamis at the coast of the Balearic Islands, *Physics and Chemistry of the Earth, Parts A/B/C*, 34(17), 938 – 947, doi:https://doi.org/10.1016/j.pce.2009.10.001, meteorological Tsunamis: Atmospherically Induced Destructive Ocean Waves in the Tsunami Frequency Band.
- Monserrat, S., I. Vilibić, and A. B. Rabinovich (2006a), Meteotsunamis: atmospherically induced destructive ocean waves in the tsunami frequency band, *Natural Hazards and Earth System Sciences*, 6(6), 1035–1051, doi:10.5194/nhess-6-1035-2006.
- Monserrat, S., I. Vilibic, and A. B. Rabinovich (2006b), Meteotsunamis: atmospherically induced destructive ocean waves in the tsunami frequency band, *Natural Hazards and Earth System Science*, 6(6), 1035–1051.
- Monserrat, S., I. Vilibic, and A. B. Rabinovich (2006c), Meteotsunamis: atmospherically induced destructive ocean waves in the tsunami frequency band, *Natural Hazards and Earth System Science*, 6(6), 1035–1051.

- Proudman, J. (1929), The Effects on the Sea of Changes in Atmospheric Pressure, *Geophysical Supplements to the Monthly Notices of the Royal Astronomical Society*, 2(4), 197–209, doi: 10.1111/j.1365-246X.1929.tb05408.x.
- Rabinovich, A. B. (2012), *Seiches and Harbor Oscillations*, 193-236 pp., World scientific.
- Renault, L., G. Vizoso, A. Jansà, J. Wilkin, and J. Tintoré (2011), Toward the predictability of meteotsunamis in the Balearic Sea using regional nested atmosphere and ocean models, *Geophysical Research Letters*, 38(10), doi:10.1029/2011GL047361.
- Romero, R., M.Vich, and C.Ramis (2019), A pragmatic approach for the numerical prediction of meteotsunamis in Ciutadella harbour (Balearic Islands).
- Sepić, J., I. Vilibic, A. B. Rabinovich, and S. Monserrat (2015), Widespread tsunami-like waves of 23-27 June in the Mediterranean and Black Seas generated by high-altitude atmospheric forcing.
- Stergiou, I., E. Tagaris, and R. Sotiropoulou (2017), Sensitivity Assessment of WRF Parameterizations over Europe, *Proceedings, I*, 119, doi:10.3390/ecas2017-04138.
- Tintoré, J., D. Gomis Bosch, S. Alonso, and D.-P. Wang (1988), A theoretical study of large sea level oscillations in the western Mediterranean, *Journal of Geophysical Research*, 931, 10,797–10,803, doi:10.1029/JC093iC09p10797.
- Vilibic, I., S. Monserrat, A. Rabinovich, and H. Mihanović (2008), Numerical Modelling of the Destructive Meteotsunami of 15 June, 2006 on the Coast of the Balearic Islands, *Pure and Applied Geophysics*, 165(11), 2169–2195, doi:10.1007/s00024-008-0426-5.

Agraïments

Ja que en el treball de final de màster es pot incloure agraïments, m'agradaria aprofitar-ho. Primer de to vull donar les gràcies a nen Joaquin Tintoré, director del SOCIB, a nen Saül Pitarch i a tota la gent del SOCIB per haver-me donat l'oportunitat de poder treballar amb ells durant tot el curs del màster. Ha estat una experiència innovadora i gratificant al mateix temps, ja que he pogut viure la vida d'investigador durant un any.

També donar les gràcies en particular a l'equip de Modelling and Forecasting facilities. Gràcies a nen Baptiste per la paciència i l'ajuda que m'ha donat quan l'he necessitat. També donar les gràcies a nen Jaime, que sempre que he tengut problemes amb el matlab ha estat allà per donar-me un cop de mà.

Si he de donar gràcies, no puc oblidar-me mai de n'Aina, en Toni, n'Adel i en Dani. Sense ells no seria possible aquest màster, ni tan sols la carrera. Moltes gràcies per tota l'ajuda que m'heu donat tant en temes acadèmics com en temes personals. Sou els millors.

Vull donar també les gràcies a la meva família. Sempre estan allà, són un pilar fonamental per a la meva vida i també ho han estat en els moments difícils de l'any. Hagués estat impossible realitzar aquest treball sense el seu suport.

Finalment donar les gràcies a na Natàlia. La que possiblement ha hagut d'aguantar-me més que ningú. Per la seva paciència amb jo quan no estava de bon humor. Gràcies per fer-me riure quan les coses del màster no sortien. Però sobretot, gràcies per estar sempre al meu costat.